بسم الله الرحمن الرحيم

Sudan University of Science & Technology

College of Engineering

School of Electrical & Nuclear Engineering

Study of wind farm turbine based on doubly fed induction generator

دراسه توربينات الرياح التي تعتمد علي المولد الحثي ثنائي التغذيه

A project Submitted In Partial Fulfillment for the Requirement of The Degree of B.Sc. (Honor) In Electrical Engineering

Prepared By:

1- **Eissa Altegany Eissa Omar**

2- **Munzer Osman Ibraheem Osman**

3- **Moaid Bakhet Ahmed Bakhet**

4- **Mohammed kamal Mohammed Alabaid**

Supervision by:

Dr.Nagm eldeen Abdo Mustafa Hassanain

October 2015

الآيـة

قال تعالى:

(يَا أَيُّهَا الَّذِينَ آمَنُوا إِذَا قِيلَ لَكُمْ تَفَسَّحُوا فِي الْمَجَالِسِ فَافْسَحُوا يَفْسَحِ اللَّهُ لَكُمْ ۖ وَإِذَا قِيلَ انْشُزُوا فَانْشُزُوا يَرْفَعِ اللَّهُ الَّذِينَ آمَنُوا مِنْكُمْ وَالَّذِينَ أُوتُوا الْعِلْمَ دَرَجَاتٍ ۚ وَاللَّهُ بِمَا تَعْمَلُونَ خَبِيرٌ)

الآية (11) سورة المجادلة

DEDICATION

To our parents who always inspiring and devising us, nothing

Of this could be done without them, May Allah saves them

Always for us.

To our supervisor **Dr.Nagm eldeen Abdo Mustafa Hassanain**,

Who always donates us his knowledge and never disappointing

Us or let us down. To our dears, all of our family members who

Always be there when we need them.

To our best friends & colleagues who are always with us step

By step, supports us to go forward.

To everyone who is an integral part of our support group, we

Dedicate this work.

ACKNOWLEDGEMENT

The greatest thanks to Allah always before and after.

We would like to express our deep gratitude to everyone who

Helps us throughout this work at any step of it.

Most grateful and appreciation to our supervisor:

Dr.Nagm eldeen Abdo Mustafa Hassanain

For their expertise support and endless valuable advices which

Guided us throughout this work and our engineering career life.

We also would like to thank all of our teachers in the school of

Electrical and nuclear engineering for all the help & knowledge

That they gave to us.

Abstract

The aim of this project is to present the complete modeling and simulation of wind turbine driven doubly-fed induction generator which feeds ac power to the utility grid. For that, two pulse width modulated voltage source converters are connected back to back between the rotor terminals and utility grid via common dc link. The grid side converter controls the power flow between the DC bus and the AC side and allows the system to be operated in sub-synchronous and super synchronous mode of operation. The proper rotor excitation is provided by the machine side converter. The complete system is modeled and simulated in the MATLAB Simulink environment in such a way that it can be suited for modeling of all types of induction generator configurations. The model makes use of rotor reference frame using dynamic vector approach for machine model.

مستخلص

الهدف من هذا المشروع هو محاكاه ودراسه توربينات الرياح التي تعتمد في تشغيلها علي محرك حثي ثلاثي الطور ثنائي التغذيه والذي يقوم بإمداد الشبكه بالطاقه الكهربائيه, يتم التحكم في المولد بواسطه الكترونات القدره التي تعتمد في تشغيلها علي تعديل عرض النبضه وتكون موصله بين العضو الدوار والشبكه الكهربائيه بواسطه خط ربط تيار مباشر.

المبدلات الموصله في جانب الشبكه تقوم بالتحكم في إنسياب القدره بين خط ربط التيار المباشر وبقيه الشبكه, وتسمح للنظام بأن يعمل بسرعه أقل من السرعه التزامنيه أو بسرعه أعلي من السرعه التزامنيه. أما المبدلات التي تكون في جانب العضو الدوار فتقوم بالتحكم في عمليه إثاره المولد.تمت عمليه المحاكاه والنمزجه الكليه بإستخدام برنامج الماتلاب بطريقه مناسبه لتمثيل كل انواع المولدات الحثيه وذلك باستخدام النمازج الديناميكيه.

LIST OF FIGURES

LIST OF SYMPOLES

WG	wind generator
DFIG	doubly-fed induction generator
WECS	Wind Energy Conversion System
PWM	Pulse-Width Modulation
CO_2	Carbon Dioxide
DC	Direct Current
AC	Alternating Current
A	Cross-Sectional Area of the Wind That Crossed the Blades
V	is the wind speed
ρ	is the air density
COTS	Commercial-Off-the-Shelf
GSC	Grid Side Converter
HAWT	Horizontal-Axis Wind Turbine
HIL	Hardware-in-the-Loop
IEEE	Institute of Electrical and Electronics Engineers
IGBT	Insulated-Gate Bipolar Transistor
KV	Kilo Volt
MVAR	Megavolt Ampere Reactive
MW	Mega Watt
PI	Proportional – Integral
PM	Permanent Magnet
PS	Pure Simulation

Pu	Per Unit
R	Blade Radius of Wind Turbine
RCP	Rapid Control Prototyping
RSC	Rotor Side Converter
RTS	Real Time Simulation
RT-LAB	Real-Time Laboratory
S	Slip of Machine
Ts	Step Size
VAWT	Vertical-Axis Wind Turbine
WTG	Wind Turbine Generator
WG	Wind Generator
C_p	Power Coefficient
P_m	Power of Wind Turbine Rotor
$P_{Available}$	Power Available
β°	Blade Pitch Angle
λ	Tip Speed Ratio
ω_r	Rotor Angular Speed
P_e	electrical power output
η_e	Efficiency of Electrical Generator
η_m	Overall Mechanical Efficiency of Transmission
Tm	mechanical torque
T_{haft}	shaft torque
H	Inertia constant

T_r	Rotor torque
m_i	modulation index
Lm	magnetizing inductance
LC	Inductance capacitance filter

CHAPTER ONE
INTRODUCTION

1.1 Introduction

In recent years, global warming has become the center of attention due to its negative impact on the environment. However, many studies have been made to reduce the emissions of carbon dioxide (CO_2) which is the main cause of greenhouse gases emission. According to these studies, using biofuel as the source for generating electricity is the primary source of CO_2 emissions in the world. The CO_2emissions from the electricity generation sector is approximately 40% worldwide, followed by transportation, industry, and other sectors.

The studies also emphasized the need to migrate towards a more efficient method of generating electricity to reduce the impact of global warming issues. Integrating renewable energy into the electricity generation sector could save the world from a serious problem due to greenhouse gases produced from power plants.

The adaptation of reliable renewable energy into the power grid has dramatically developed in recent years to become more reliable with better power generation quality. Figure 1.1 depicts the projection of the annual growth rates of energy consumption by energy source from 2005 to 2035 as determined by the U.S. Energy Information Administration's International Energy Outlook [2]. Figure 1.1 illustrated that the amount of global hydroelectric and other renewable electric generating capacity will rise 2.7% per year through 2035 (2,372 gigawatts), more than any other electricity generating source, because of the higher oil costs and climate change concerns which encourage to switch to cheaper and cleaner generating fuels [2].

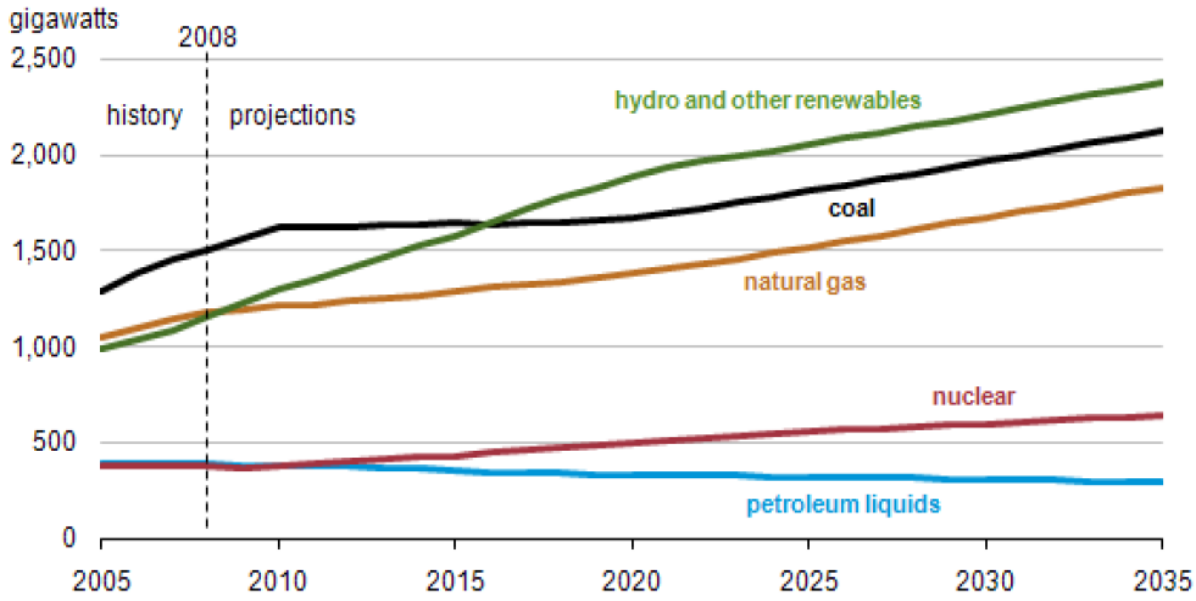

Figure 1.1 Global installed power generation capacity by energy source [2].

As shown in figure 1.2, wind power is one of the fastest growing renewable energy worldwide between 2010 and 2035. By 2020, wind power would account for more than 12% of the world's total installed capacity

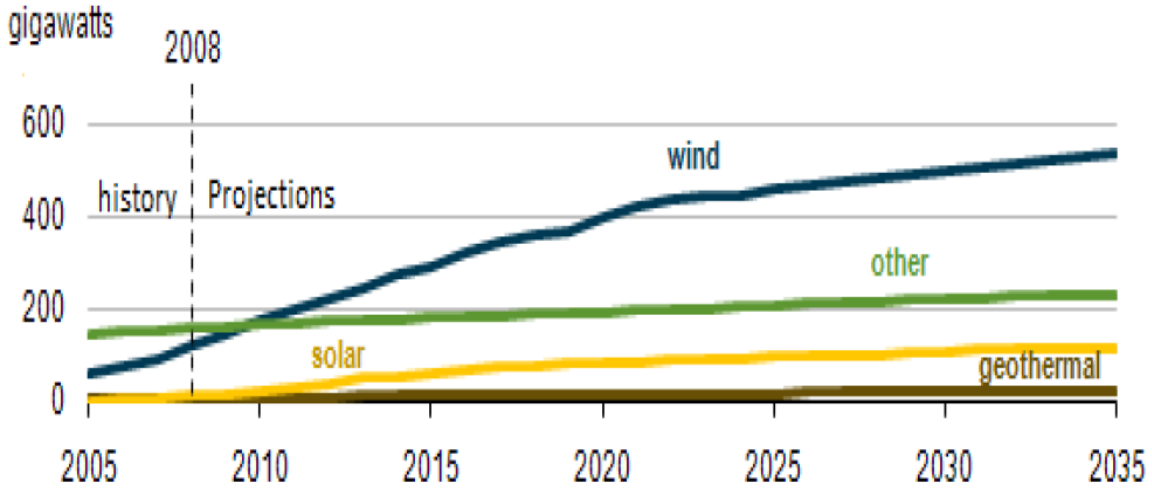

Figure1.2: Global installed power generation capacity by renewable source

The mechanical nature of wind energy has allowed the use of several types of wind generator (WG) such as squirrel cage induction generator (fixed speed), wound-rotor induction generator with adjustable external rotor resistance, doubly-fed induction generator, and induction machine with full converter interface. The last three types are classified as variable-speed wind turbines which are preferable over traditional fixed speed wind turbines due to their

higher energy yields, extracting power in a perfect way, lower power fluctuations, and less mechanical stress. The doubly-fed induction generators (DFIG) are currently the most popular wind generators in the market among variable-speed wind turbines because of their high energy efficiency and controllability .The general shape for the DFIG is that the DFIG stator side is connected to the grid directly while the rotor windings are connected to the grid via AC/DC/AC IGBT power converter. The rotor side comparing to the stator side transfers one third (1/3) of the output power to the grid. Therefore, the converter rating is lower than the generator rating. The impact of penetration small scale of the wind turbine generators on the power system stability is minimal. Unlike the conventional design of a power distribution system, WGs are designed to be in close proximity to the load. Doing so, this design attracted many benefits to the existing grid system, such as; reducing power losses from the line, increasing the reliability of the grid, and reducing the cost of operation. However, when the penetration of the small scale the wind turbine generators increases, the dynamic performance of power system can be affected. Therefore, a virtual plant model is needed to investigate and test the impacts of the integration of wind farms into a power system under different conditions to overcome any problem that might happen on a physical plant. One of the means to build a virtual plant model is to use the simulation tool. Most of existing studies on the simulation pertinent to wind power mainly focus on off-line simulation which has to go through a long research period with low accuracy. By contrast, an advanced real-time simulation platform, the math work Laboratory (*MATLAB*) developed simulation environment , which can shorten the research period and give results that come close to the physical system .[2]

1.2 Problem Statement

Because the world is getting hotter ,in fact by 1 C on land over the last 100 years ,and the scientific opinion is that the human activities particularly the emission of gasses ,are the cause.

And if we are to tackle climate change its clear we need to move away from burning limited fossil fuel reserves more sustainable and renewable source of energy.

1.3 Objective:-

The objectives of this project are summarized as follows:

1. Modeling of a variable speed wind energy conversion system (WECS) including a doubly fed induction generator as an electrical power generation unit.
2. Controlling and improving the performance of a doubly fed induction generator driven by a wind turbine system during wind speed variations based on field orientation control principle.
3. Investigating the effect of the grid faults on the dynamic performance of variable speed wind-driven doubly fed induction generator connected to the grid.
4. Enhancing the capability of a wind driven doubly fed induction generator to fault ride through during grid faults.

1.4 Methodology

In order to achieve these objectives the following Steps: -

- Study the wind energy, aerodynamic conversion and how to extract the maximum power at variable wind speed.
- Study the models of wind turbine and DFIG and the operation of wind farm based on double fed induction generator.
- According to these models, a simulink program has been developed to analyze the wind farm operation.

1.5 project Outline

This project consists of five chapters. In chapter 1, the background to the study has been reviewed. Chapter 2 shows general theoretical perspective of wind turbines in general and focuses more in depth on the DFIG wind turbine. In chapter 3, we presents the models DFIG and wind turbine used to model and execute the Simulink model under the MATLAB environment. Chapter 4 presents a detailed 9-MW wind farm model in the configuration. Moreover, it describes in details the system result of the different case of studies. Finally, the conclusion and suggestions for future studies are presented in chapter 5.

CHAPTER TWO
LITRATURE REVIEW

2.1 Introduction

The first use of wind power was to sail ships in the Nile some 5000 yr ago. Many civilizations used wind power for transportation and other purposes, The Europeans used it to grind grains and pump water in the 1700s and 1800s. The first wind mill to generate electricity in the rural U.S. was installed in 1890. An experimental grid connected turbine with as large a capacity as 2 MW was installed in 1979 on Howard Knob Mountain near Boone, NC, and a 3-MW turbine was installed in 1988 on Berger Hill in Orkney, Scotland. Today, even larger wind turbines are routinely installed, commercially competing with electric utilities in supplying economical, clean power in many parts of the world. The average turbine size of wind installations was 300 kW until the early 1990s.New machines being installed are in the 1- to 3-MW capacity range. Wind turbines of 5-MW capacity has been fully developed and are under test operation in several countries, including the U.S. is a conceptual layout of a modern multi mega wind tower suitable for utility-scale applications.1Improved turbine designs and plant utilization have contributed to a decline in large-scale wind energy generation costs from 35 cents/kWh in 1980 to 3 to 4cents/kWh in 2004 at favorable locations. At this price, wind energy has become the least expensive new source of electric power in the world, less expensive than coal, oil, nuclear, and most natural-gas-fired plants, competing with these traditional sources on its own economic merit. Hence, it has become economically attractive to utilities and electric cooperatives, with 30% growth from 1993to 2003. Worldwide, over 40,000 MW of wind capacity has been installed, and more than 100,000-MW capacity by 2015 is predicted. Major factors that have accelerated the development of wind power technology are as follows:

- High-strength fiber composites for constructing large, low-cost blades
- Falling prices of the power electronics associated with wind power systems
- Variable-speed operation of electrical generators to capture maximum energy
- Improved plant operation, pushing the availability up to 95%
- Economies of scale as the turbines and plants are getting larger in size
- Accumulated field experience (the learning-curve effect) improving the Capacity factor up to 40%. [1]

2.2 Wind Energy Conversion System

Wind energy conversion system (WECS) is the overall system that converts the wind energy into useful electrical power through a mechanical power. The WECS consists of three major aspects: aerodynamic, mechanical and electrical aspect. The major parts included in the mechanical and the electrical power conversion of a typical wind turbine system are shown in figure 2.1 [2].

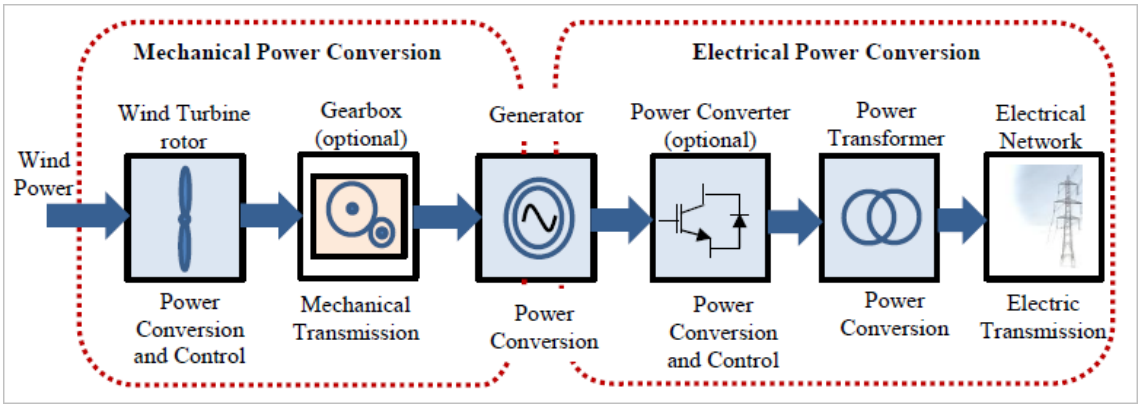

Figure 2.1 Block diagram showing the components of WECS connected to grid.

Modern wind turbines are generally classified into two basic groups:

The horizontal-axis wind turbines (HAWT) and the vertical-axis wind turbines (VAWT). Currently, most of the wind turbines using in the market are from HAWT type. It named HAWT because its shaft rotates on an axis parallel to the ground level. The HAWTs are divided into downwind horizontal axis wind.

Turbines and upwind horizontal axis wind turbines. As shown in figure 2.2, the rotor blades of the downwind turbines are stroked by wind from the back side. On the other hand, the rotor blades of the upwind turbine are facing the wind directly. This type requires a complex yaw control systems to keep the blades facing into the wind, but it operates more smoothly and delivers more power comparing to the other type. For these reasons, the majority of modern wind turbines are from the upwind type. Therefore, most of the technologies described in this thesis are related to three blades upwind horizontal axis wind turbines (HAWTs). [2]

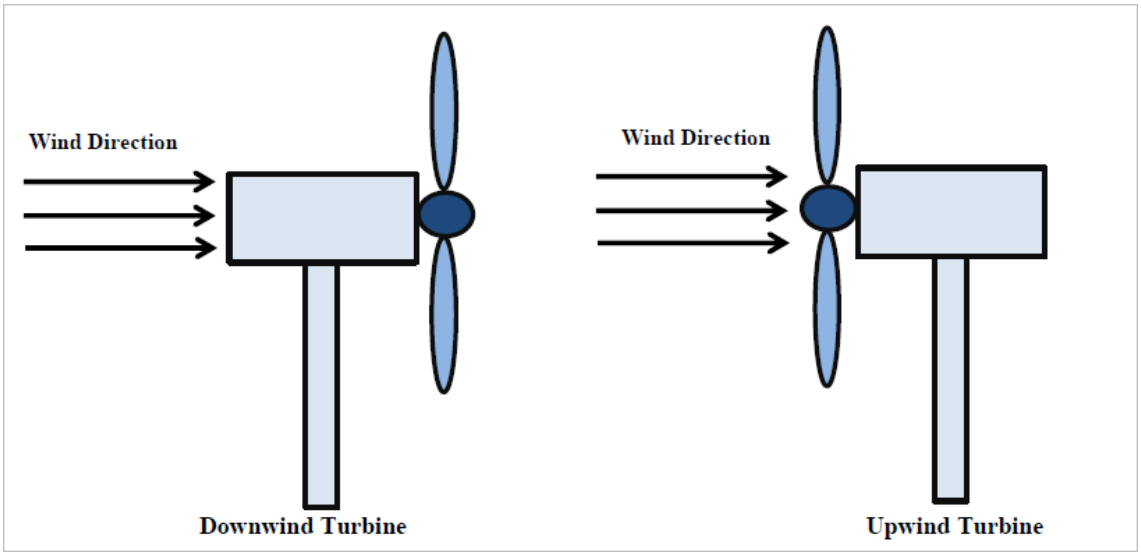

Figure 2.2 Downwind turbine and upwind turbine.

2.3 Basic Components of a Wind Turbine

The main mechanical and electrical components of a wind turbine system are shown in figure 2.3. A typical HAWT made up of the following parts: rotor, drive train, nacelle, mainframe, tower and foundation. The rotor is formed by blades and hub and this part is responsible to extract the wind energy and convert it into mechanical energy. For drive train, it is formed by, low-speed shaft, gearbox, electrical generator, and high-speed shaft. This group is using the mechanical energy from the rotor and converts it into electricity through the

electrical generator. For nacelle and main-frame, they are formed by housing, bedplate, and yaw system. Also, the transformer and power electronics converters can be added to last group if possible. The yaw system is used to allow the rotor facing the wind direction to extract maximum power. [2]

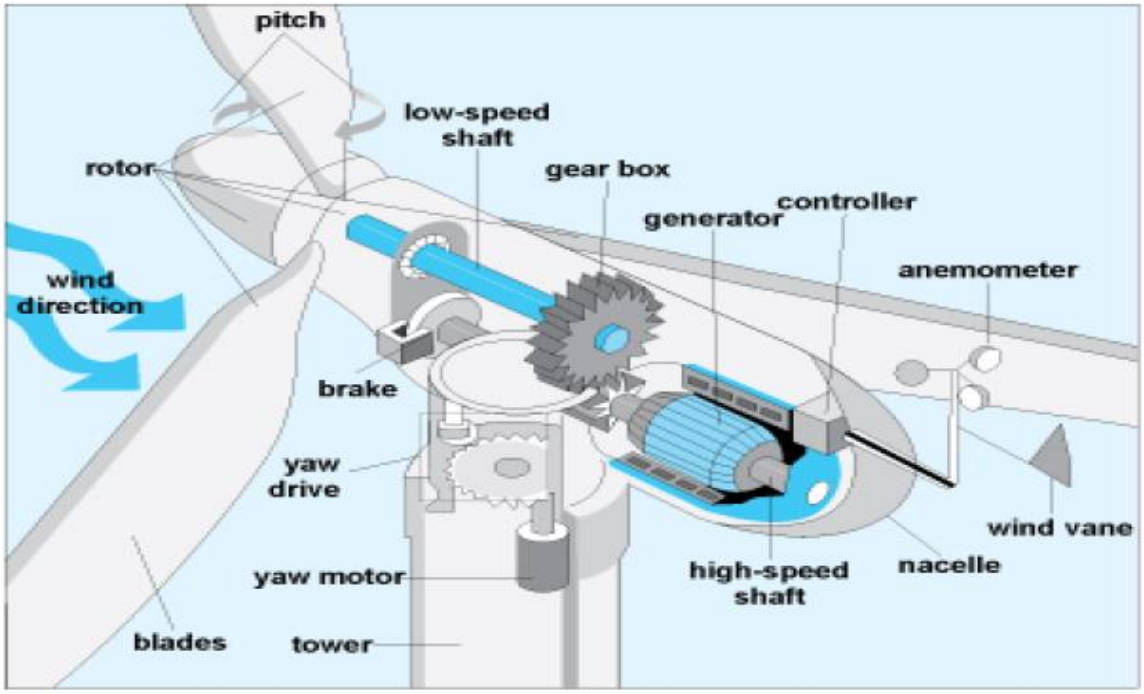

Figure 2.3 Typical HAWT components [4].

2.4 Wind Turbine Generators

At the present time, there are four types of construction modes wind turbine generators

(WTGs) used currently in the market, based on the grid connection:

- Squirrel cage induction generator.
- Wound-rotor induction generator with adjustable external rotor resistance.
- Doubly-fed induction generator.
- Induction machine with full converter interface.

In conventional (singly-fed) induction generators, when the generator rotor rotates due to the prime mover, the static magnetic field created by the dc

current fed into the rotor windings rotates at same speed as the rotor. As a result of changing magnetic flux, this will induce the three-phase voltage at the stator side. Same operating principles can be applied in a DFIG except that the dc current fed into the generator rotor winding is not static as in the conventional induction generator, but it is creating using three-phase current with adjustable frequency via the power converter . The doubly-fed induction generators (DFIGs) are the most popular wind generators due to their high energy efficiency and controllability. As shown figure 2.4 the DFIG stator side connected to the grid directly via a power transformer and the rotor windings connected to the grid via AC/DC/AC IGBT power converter and a power transformer. This converter comparing to the stator side transfers one-third (1/3) of the output power to the grid. Therefore, the converter rating is lower than the generator rating [6].

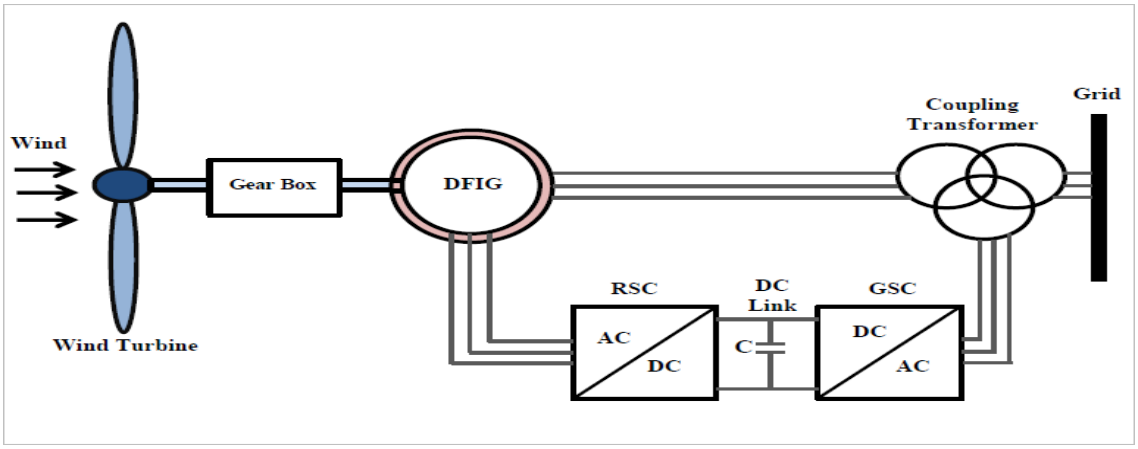

Figure 2.4 Doubly-fed induction generator

2.5 Theory of wind turbines

As mentioned at the beginning of this chapter that the main role of the wind turbines is to extract energy from the wind. Therefore, the power available ($P_{Available}$) that can be extracted from the wind is given by.

$$P_{Available} = \frac{1}{2} . \rho . A . V^3 \qquad (2.1)$$

Where

ρ is the air density (kg /m^3) .

A is the cross-sectional area of the wind crossed the blades (m^2).

V is the wind speed (m/ s).

A perfect wind turbine cannot extract all the power available in the wind. The power actually captured by the wind turbine rotor (P_m) is defined by the power coefficient C_p(or efficiency coefficient) which is the ratio between the power extracted and the available power in the wind.

$$C_p = \frac{P_m}{P_{Available}} \tag{2.2}$$

The maximum theoretical value of the efficiency coefficient ($C_{p,max}$) is 0.593, which is commonly known as the Betz limit. Actual efficiency coefficient is less than this limit due to various aerodynamic and mechanical losses. By substituting equation (2.1) into equation (2.2), it will give the mechanical power that can be extracted by the wind turbine which is a function of the power coefficient (C_P) and the available wind power:

$$P_m = \frac{1}{2} . C_P . \rho . A . V^3 = \frac{1}{2} . C_P . \rho . \pi . R^2 . V^3 \tag{2.3}$$

Generally, the power coefficient (C_P) is a function of tip speed ratio (λ) and blade pitch angle (β°).

As illustrated in figure (2.5), there is a maximum value for the power coefficient with respect to tip speed at various values of the pitch angle (β°). The tip speed ratio is given by:

$$\lambda = \frac{\omega_r . R}{V} \tag{2.4}$$

Where

ω_r is rotor angular speed (rad/s).

R is the blade radius of the wind turbine (m^2).

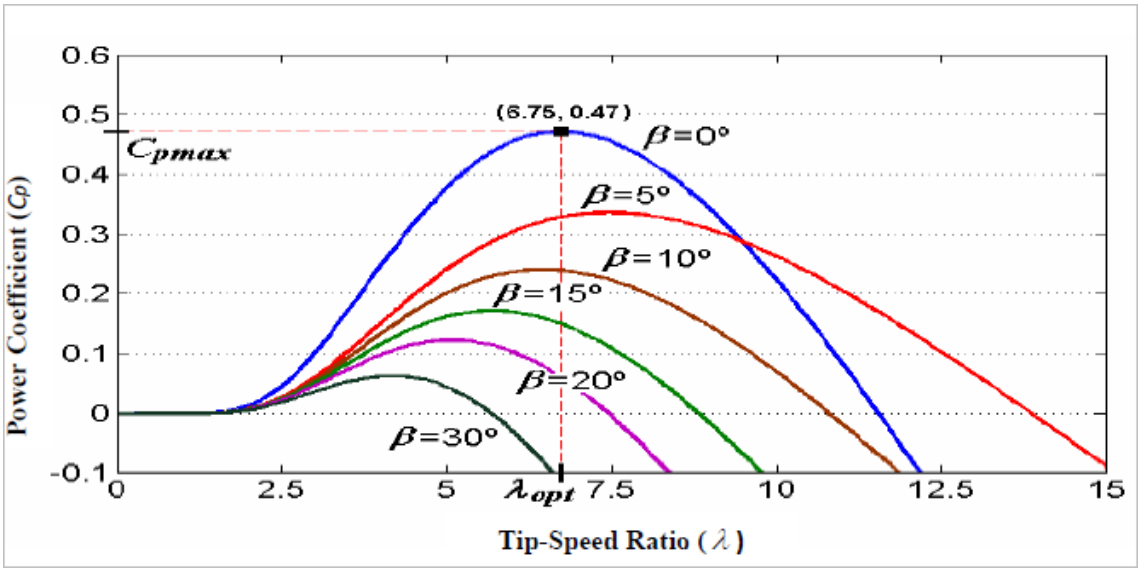

Figure 2.5 Characteristics function of $C_P$vs. λ , at various pitch angle values

Figure 2.6 shows the mechanical power versus the rotating speed of the generator with no blade pitch angle control ($\beta = 0^{\circ}$) at various wind speeds. It is observed that the operation of the Wind generator must follow a specific point of the rotor speed for each wind speed to maximize the mechanical power to get the maximum value of the wind power coefficient ($C_{p,max}$). Thus, the maximum mechanical power that can be continuously extracted from the low and the medium wind can be achieved by control the rotate speed of the generator to tracking the maximum power point (MPP tracking control or MPPT) for each wind speed as depicted by dotted line in figure (2.6).

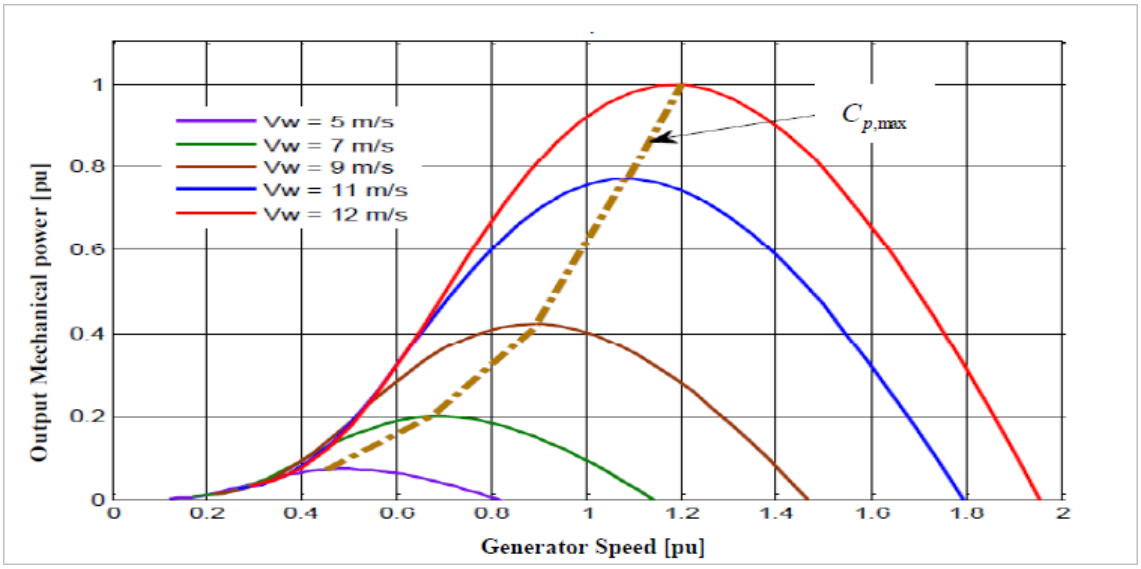

Figure 2.6: Mechanical power versus rotor speed curves [8].

The aerodynamic torque captured by the rotor of the wind turbine is described as.

$$T_r = \frac{P_m}{\omega_r} = \frac{\frac{1}{2} . C_P . \rho . A . V^3}{\omega_r} \quad (2.5)$$

In large wind turbines, the mechanical power (P_m) expressed in equation 2.3 is not directly connected to the generator, but is usually coupled through a transmission or gear box. Thus, as shown in figure 2.7, the electrical power output (P_e) that is connected to the grid or auxiliary circuits can be expressed as:

$$P_e = \eta_m . \eta_e . \frac{1}{2} . C_P . \rho . A . V^3 \quad (2.6)$$

Where

η_m is the overall mechanical efficiency of the transmission.

η_e is the overall efficiency of the electrical generator.

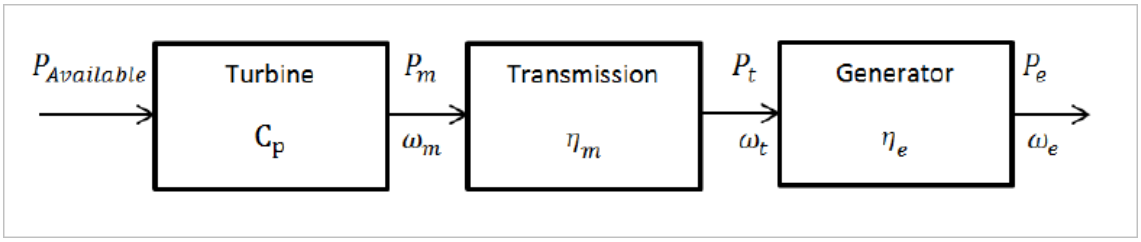

Figure 2.7 Wind electrical system.

2.6 Wind Turbine Power Curves Characteristics

Each wind turbine performance can be estimated by the power curve which is usually given by the manufacturer of the wind turbine. The power curve, which is the function of the estimated power output to wind speed, is used to measure the total wind power protection by the wind turbine. There are three distinct points to any power curve of a variable-speed variable pitch wind turbine as illustrated in figure 2.8 [4]:

- Cut-in wind speed (2-4 m/s): the blades start to rotate and consequently the wind turbine generator begins to generate power to supply the load.
- Rated wind speed (11 -20 m/s): after the wind speed increasing above the cut-in speed point, the wind turbine generator starts to produce more

power which is proportional to the cube of the wind speed. By increasing the wind speed further, the output power of the generator will increase until the wind speed reaches the rated wind speed at which the output power of the generator is regulated to its rated power

- Cut-out or furling wind speed (20-25 m/s): at some point when the wind increase above the rated wind speed range in which the wind turbine must be shut down to avoid mechanical damage due to the high wind speed. This is achieved by adjusting the blade pitch angle and by using brakes.

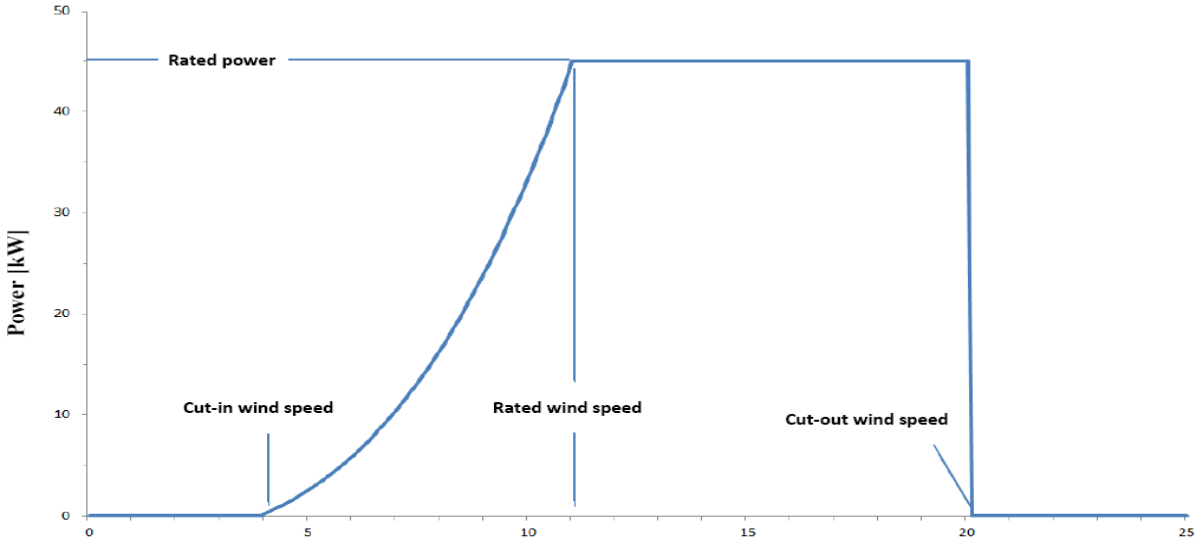

Figure 2.8 Wind turbine power curve characteristics [2].

CHAPTER THREE

MATHEMATICAL MODELS

3.1 Wind Turbine Model

Many wind turbines are equipped with fixed frequency induction generators. Thus the power generated is not optimized for all wind conditions. To operate a wind turbine at its optimum at different wind speeds, the wind turbine should be operated at its maximum power coefficient (Cp-optimum = 0.3-0.5). To operate around its maximum power coefficient, the wind turbine should be operated at a constant tip-speed ratio, which is proportional to ratio of the rotor speed to the wind speed. As the wind speed increases, the rotor speed should follow the variation of the wind speed. In general, the load to the wind turbine is regulated as a cube function of the rotor rpm to operate the wind turbine at the optimum efficiency. The aerodynamic power generated by wind turbine can be written as: [3]

$$P_m = 0.5\rho\, AC_p\left(\lambda, \beta\right) V^3 \tag{3.1}$$

Where the aerodynamic power is expressed as a function of the specific density (ρ) of the air, the swept area of the blades (A) and the wind speed (V_w), to operate the wind turbine at its optimum efficiency (Cp-optimum), the rotor speed must be varied in the same proportion as the wind-speed variation. If we can track the wind speed precisely, the power can also be expressed in terms of the rotor speed. [3]

$$P_m = K_P\omega^3 \tag{3-2}$$

The power described by equation [3.2] will be called P_{ideal}.

The power coefficient C_p as a function of Tip-Speed Ratio (TSR) λ, where, λ is given in terms of rotor speed, ω(rad/s), wind speed, V_w(m/s), and rotor radius, R (m)

$$\lambda = \frac{R\omega}{V} \tag{3.3}$$

Wind turbine power coefficient, C_p is dependent upon λ. If pitch angle, β, is incorporated, C_p becomes a function of λ and

$$C_p(\lambda,\ \beta) = 0.5176\left(\frac{116}{\lambda_i} - 0.4\times\beta - 5\right)e^{-\frac{21}{\lambda_i}} + 0.0068\times\lambda_i$$

(3.4)

Where

$$\frac{1}{\lambda_i} = \left(\frac{1}{(\lambda+0.08\beta)}\right) - \left(\frac{0.035}{(\beta^3+1)}\right) \qquad (4.5)$$

When the wind speed is increased the maximum power extracted from the wind is increased for the same turbine speed. The equations of the torque of the wind turbine are [12].

$$T_m = \frac{p_m}{\omega} \qquad (3.6)$$

$$\frac{T_m - T_{shaft}}{2H} = \frac{dw}{dt} \qquad (4.7)$$

Where

$\boldsymbol{T_m}$= mechanical torque, $\boldsymbol{T_{haft}}$ =shaft torque, $\boldsymbol{H}$=Inertia constant, $\boldsymbol{p_m}$= mechanical power and $\frac{dw}{dt}$ is the differential of Turbine rotor speed.

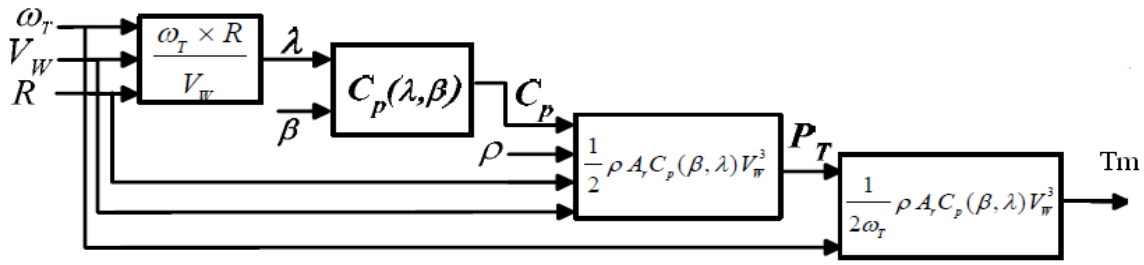

Figure (3.1) represent the wind turbine model.

3.2 Induction machine Model

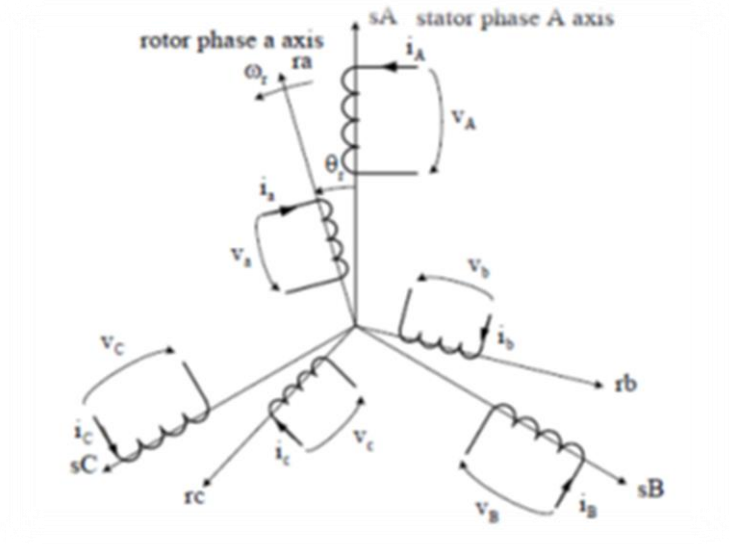

Figure 3.2: Three phase induction machine

The voltages equations of three phase induction machine are:

$$[V]=[R]\cdot[I]+\frac{d[\psi]}{dt} \tag{3.8}$$

$$[\psi]=[L]\cdot[I] \tag{3.9}$$

Where

- $[V]=[V_A\ V_B\ V_C\ V_a\ V_b\ V_c]^t \rightarrow$ are the voltages applied to each stator and rotor phases.
- $[I]=[I_A\ I_B\ I_C\ I_a\ I_b\ I_c]^t \rightarrow$ are the currents in each stator and rotor phases.
- $[\psi]=[\varphi_A\ \varphi_B\ \varphi_C\ \varphi_a\ \varphi_b\ \varphi_c]^t \rightarrow$ are the fluxes linked with each stator and rotor.
- $[R]$ is the resistance matrix and $[L]$is the inductance matrix.

The inductance and resistance matrix are defind as:

$$[L]=\begin{bmatrix} L_s & -0.5M_S & -0.5M_S & M_{sr}f_1 & M_{sr}f_2 & M_{sr}f_3 \\ -0.5M_S & L_s & -0.5M_S & M_{sr}f_3 & M_{sr}f_1 & M_{sr}f_2 \\ -0.5M_S & -0.5M_S & L_s & M_{sr}f_2 & M_{sr}f_3 & M_{sr}f_1 \\ M_{sr}f_1 & M_{sr}f_3 & M_{sr}f_2 & L_r & -0.5M_r & -0.5M_r \\ M_{sr}f_2 & M_{sr}f_1 & M_{sr}f_3 & -0.5M_r & L_r & -0.5M_r \\ M_{sr}f_3 & M_{sr}f_2 & M_{sr}f_1 & -0.5M_r & -0.5M_r & L_r \end{bmatrix} \quad (3.10)$$

$$[R]=\begin{bmatrix} R_s & 0 & 0 & 0 & 0 & 0 \\ 0 & R_s & 0 & 0 & 0 & 0 \\ 0 & 0 & R_s & 0 & 0 & 0 \\ 0 & 0 & 0 & R_r & 0 & 0 \\ 0 & 0 & 0 & 0 & R_r & 0 \\ 0 & 0 & 0 & 0 & 0 & R_r \end{bmatrix} \quad (3.11)$$

where:

$L_s = L_{\sigma s} + M_s \rightarrow$ stator self-inductance

$L_r = L_{\sigma r} + 1.5M_r \rightarrow$ rotor self-inductance

$L_{\sigma s}, L_{\sigma r} \rightarrow$ stator and rotor leakage indactance

$M_s, M_r \rightarrow$ stator and rotor mutual indactance

$M_{sr} \rightarrow$ stator-rotor mutual inductance

The coefficients f_1, f_2, f_3

$$f_1 = \cos\theta_r \ , f_2 = \cos\left(\theta_r + \frac{2\pi}{3}\right), f_3 = \cos\left(\theta_r - \frac{2\pi}{3}\right) \quad (3.12)$$

All these in inductances can easily be measured a wound rotor induction machine. For squirrel-cage induction machines, these inductances can normally be estimated from no-load and locked rotor tests. Referring the rotor parameters to stator the inductances become equals [12]:

$$M_s = M_r = M_{sr} \quad (3.13)$$

The impudence matrix is defined as:

$$[Z]=\begin{bmatrix} R_s+L_sP & -0.5PM_S & -0.5PM_S & M_{sr}Pf_1 & M_{sr}Pf_2 & M_{sr}Pf_3 \\ -0.5PM_S & R_s+L_sP & -0.5PM_S & M_{sr}Pf_3 & M_{sr}Pf_1 & M_{sr}Pf_2 \\ -0.5PM_S & -0.5PM_S & R_s+L_sP & M_{sr}Pf_2 & M_{sr}Pf_3 & M_{sr}Pf_1 \\ M_{sr}Pf_1 & M_{sr}Pf_3 & M_{sr}Pf_2 & R_r+L_rP & -0.5PM_r & -0.5PM_r \\ M_{sr}Pf_2 & M_{sr}Pf_1 & M_{sr}Pf_3 & -0.5PM_r & R_r+L_rP & -0.5PM_r \\ M_{sr}Pf_3 & M_{sr}Pf_2 & M_{sr}Pf_1 & -0.5PM_r & -0.5PM_r & R_r+L_rP \end{bmatrix} \quad (3.14)$$

The transformation of the 3-phase induction machine to two phase machine is done by using the phase transformation matrix C_1 and commutater transformation C_2 as follows:

$$C_1=\sqrt{\frac{2}{3}}\begin{Vmatrix} \frac{1}{\sqrt{2}} & 1 & 0 \\ \frac{1}{\sqrt{2}} & -\frac{1}{2} & \frac{\sqrt{3}}{2} \\ \frac{1}{\sqrt{2}} & -\frac{1}{2} & -\frac{\sqrt{3}}{2} \end{Vmatrix} \quad (3.15)$$

$$C_2=\begin{Vmatrix} \sin\theta & \cos\theta \\ \cos\theta & -\sin\theta \end{Vmatrix} \quad (3.16)$$

✓ **The stator is not requires a transformation by C_2**

The new impedance matrix after applied C_1

$$[Z]'=\begin{bmatrix} R_s+L_sP & 0 & M\,P\cos\theta & M\,P\sin\theta \\ 0 & R_s+L_sP & M\,P\sin\theta & -M\,P\cos\theta \\ M\,P\cos\theta & M\,P\sin\theta & R_r+L_rP & 0 \\ M\,P\sin\theta & -M\,P\cos\theta & 0 & R_r+L_rP \end{bmatrix} \quad (3.17)$$

The new impedance matrix after applied C_2 to the rotor only

$$[Z]''=\begin{bmatrix} R_s+L_sP & M\,P & 0 & 0 \\ M\,P & R_r+L_rP & \omega_m M & \omega_m L_r \\ 0 & 0 & R_s+L_sP & MP \\ -\omega_m M & -\omega_m L_r & MP & R_r+L_rP \end{bmatrix} \quad (3.18)$$

The voltages and currents equations after transformation when applied C_{12} to the rotor voltage and applied C_1 to the stator

$$[V]'' = \begin{bmatrix} V_D \\ V_d \\ V_Q \\ V_q \end{bmatrix} \tag{3.19}$$

$$[I]'' = \begin{bmatrix} I_D \\ I_d \\ I_Q \\ I_q \end{bmatrix} \tag{3.20}$$

The new voltage equation of the induction machine in dq-model:

$$\begin{bmatrix} V_D \\ V_d \\ V_Q \\ V_q \end{bmatrix} = \begin{bmatrix} R_s + L_s P & M P & 0 & 0 \\ M P & R_r + L_r P & \omega_m M & \omega_m L_r \\ 0 & 0 & R_s + L_s P & MP \\ -\omega_m M & -\omega_m L_r & MP & R_r + L_r P \end{bmatrix} \begin{bmatrix} I_D \\ I_d \\ I_Q \\ I_q \end{bmatrix} \tag{3.21}$$

3.3 Mathematical of Voltage source inverter

The three-phase two level six pulse inverter proposed corresponds to a DC/AC switching power inverter using IGBTs operated through sinusoidal PWM [7]. The mathematical equations describing and representing the operation of the voltage source inverter can be derived .by taking into account some assumptions respect to its operating conditions. For this purpose, a simplified equivalent VSI connected to the electric load is considered, also referred to as an averaged model, which assumes the inverter operation under balanced conditions as ideal, i.e. the voltage source inverter is seen as an ideal sinusoidal voltage source operating at fundamental frequency. The high frequency harmonics produced by the inverter as result of the sinusoidal PWM control techniques are mostly filtered by the low pass sine wave filters and the net

instantaneous output voltages at the point of common coupling resembles three sinusoidal waveforms phase-shifted 120º between each other. This ideal inverter is shunt-connected to the load an equivalent inductance L_s, and an equivalent series resistance R_s, and VSI semiconductors conduction losses. In the DC side, the equivalent capacitance of the one DC bus capacitor, C_d and whereas the switching losses of the VSI and power losses in the DC capacitor is considered by a parallel resistance R_p. As a result, the dynamics equations governing the instantaneous values of the three-phase output voltages in the AC side of the VSI and the current exchanged with the load can be directly derived by as follows:

$$\begin{bmatrix} v_{inva} \\ v_{invb} \\ v_{invc} \end{bmatrix} = \begin{bmatrix} R_S + sL_s \end{bmatrix} \begin{bmatrix} i_a \\ i_b \\ i_c \end{bmatrix} \tag{3.22}$$

Under the assumption that the system has no zero sequence components (operation under balanced conditions), all currents and voltages can be uniquely transformed into the synchronous-rotating orthogonal two-axes reference frame, in which each vector is described by means of its d and q components, instead of its three a, b, c components. Thus, the new coordinate system is defined with the d-axis always coincident with the instantaneous voltage vector.

Defining the d-axis to be always coincident with the instantaneous voltage vector v, yields v_d equals |v|, while v_q is null. Consequently, the d-axis current component contributes to the instantaneous active power and the q-axis current component represents the instantaneous reactive power. This operation permits to develop a simpler and more accurate dynamic model of the inverter. By applying Park's transformation stated by equation (3.17), equations (3.18) can be transformed into the synchronous rotating d-q reference frame as follows (equation (3.24)): [12]

$$K_s=\frac{2}{3}\begin{bmatrix}\cos\theta & \cos\left(\theta-\frac{2\pi}{3}\right) & \cos\left(\theta+\frac{2\pi}{3}\right)\\ -\sin\theta & -\sin\left(\theta-\frac{2\pi}{3}\right) & -\sin\left(\theta+\frac{2\pi}{3}\right)\\ \frac{1}{2} & \frac{1}{2} & \frac{1}{2}\end{bmatrix} \quad (3.23)$$

With:

$\theta=\int_0^t \omega(t)dt+\theta(0)$ Angle between the *d*-axis and the reference phase axis, and t: integration variable ω: synchronous angular speed of the network voltage at the fundamental system frequency

$$\begin{bmatrix}v_d\\ v_q\\ v_0\end{bmatrix}=K_s\begin{bmatrix}v_{inva}\\ v_{invb}\\ v_{invc}\end{bmatrix}\quad\begin{bmatrix}i_d\\ i_q\\ i_0\end{bmatrix}=K_s\begin{bmatrix}i_a\\ i_b\\ i_c\end{bmatrix} \quad (3.24)$$

Then, by neglecting the zero sequence components, equations (3.23) and (3.24) are derived.

$$\begin{bmatrix}v_{invd}\\ \\ v_{invq}\end{bmatrix}=(R_s+sL_s)\begin{bmatrix}i_d\\ \\ i_q\end{bmatrix}+\begin{bmatrix}-\omega & 0\\ 0 & \omega\end{bmatrix}L_s\begin{bmatrix}i_d\\ \\ i_q\end{bmatrix} \quad (3.25)$$

The relation between the DC side voltage V_d and the generated AC voltage V_{inv} can be described through the average switching function matrix in the d-q reference frame $S_{av,dq}$ of the inverter, as given by equation (3.25). This relation assumes that the DC capacitors voltages are balanced and equal to V_d

$$\begin{bmatrix}v_{invd}\\ \\ v_{invq}\end{bmatrix}=S_{av,dq}V_d$$

(3.26)

$$S_{av,dq}=\begin{bmatrix}S_{avd}\\ \\ S_{avq}\end{bmatrix}=\frac{1}{2}m_i\begin{bmatrix}\cos\alpha\\ \sin\alpha\end{bmatrix} \quad (3.27)$$

Being, m_i: modulation index of the voltage source inverter, m_i = (0, 1). [11]

CHAPTER FOUR

SIMULATION AND RESULTS

4.1 Introduction

A 9-MW wind farm consisting of six 1.5 MW wind turbines connected to a 25-kV distribution system exports power to a 120-kV grid through a 30-km, 25-kV feeder. A 2300V, 2-MVA plant consisting of a motor load (1.68 MW induction motor at 0.93 PF) and of a 200-kW resistive load is connected on the same feeder at bus B25. Both the wind turbine and the motor load have a protection system monitoring voltage, current and machine speed. The DC link voltage of the DFIG is also monitored.

Wind turbines use a doubly-fed induction generator (DFIG) consisting of a wound rotor induction generator and an AC/DC/AC IGBT-based PWM converter. The stator winding is connected directly to the 60 Hz grid while the rotor is fed at variable frequency through the AC/DC/AC converter. The DFIG technology allows extracting maximum energy from the wind for low wind speeds by optimizing the turbine speed, while minimizing mechanical stresses on the turbine during gusts of wind. The optimum turbine speed producing maximum mechanical energy for a given wind speed is proportional to the wind speed. For wind speeds lower than 10 m/s the rotor is running at sub synchronous speed. At high wind speed it is running at hyper synchronous speed. Open the turbine menu, select "Turbine data" and check “Display wind-turbine power characteristics". The turbine mechanical power as function of turbine speed is displayed for wind speeds ranging from 5 m/s to 16.2 m/s. The DFIG is controlled in order to follow the red curve. Turbine speed optimization is obtained between point B and point C on this curve. Another advantage of the DFIG technology is the ability for power electronic converters to generate or absorb reactive power, thus eliminating the need for installing capacitor banks as in the case of squirrel-cage induction generators.

4.2 Circuit Diagram:

This is the Simulink (Circuit) diagram for a doubly fed induction generator connected to grid side with wind turbine protection schemes involved for protection from single phase faults and ground faults. The system is connected to a 120 KV, 3 phase source which is connected to a 9MW wind farm (6 of 1.5 MW each) via. Step down transformers, fault protection and pi- transmission line. The wind-turbine model is a phasor model that allows transient stability type studies with long simulation times. In this demo, the system is observed during 50 s.

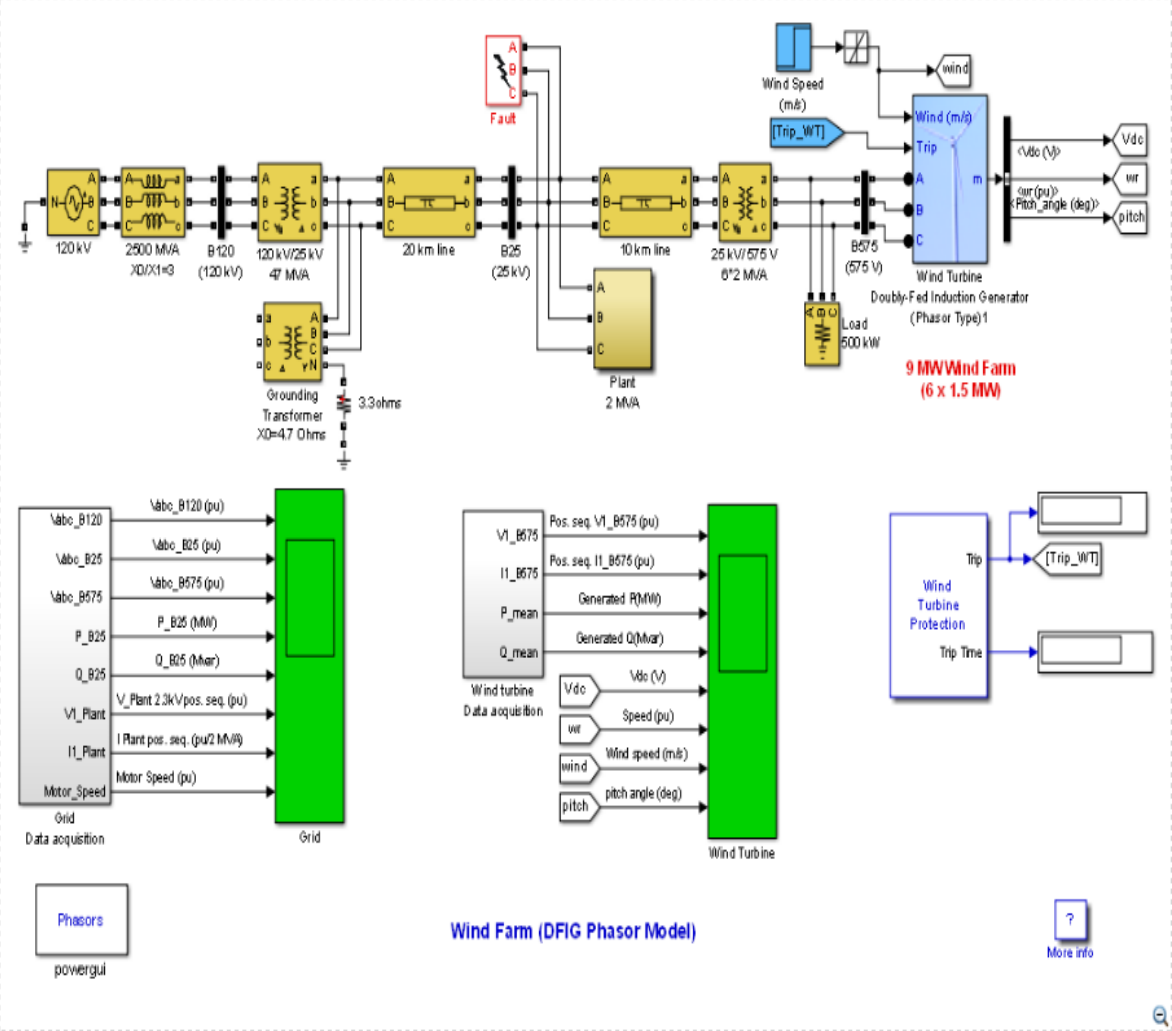

Figure (4-1): circuit diagram

4.3 Plant and Its Protection System

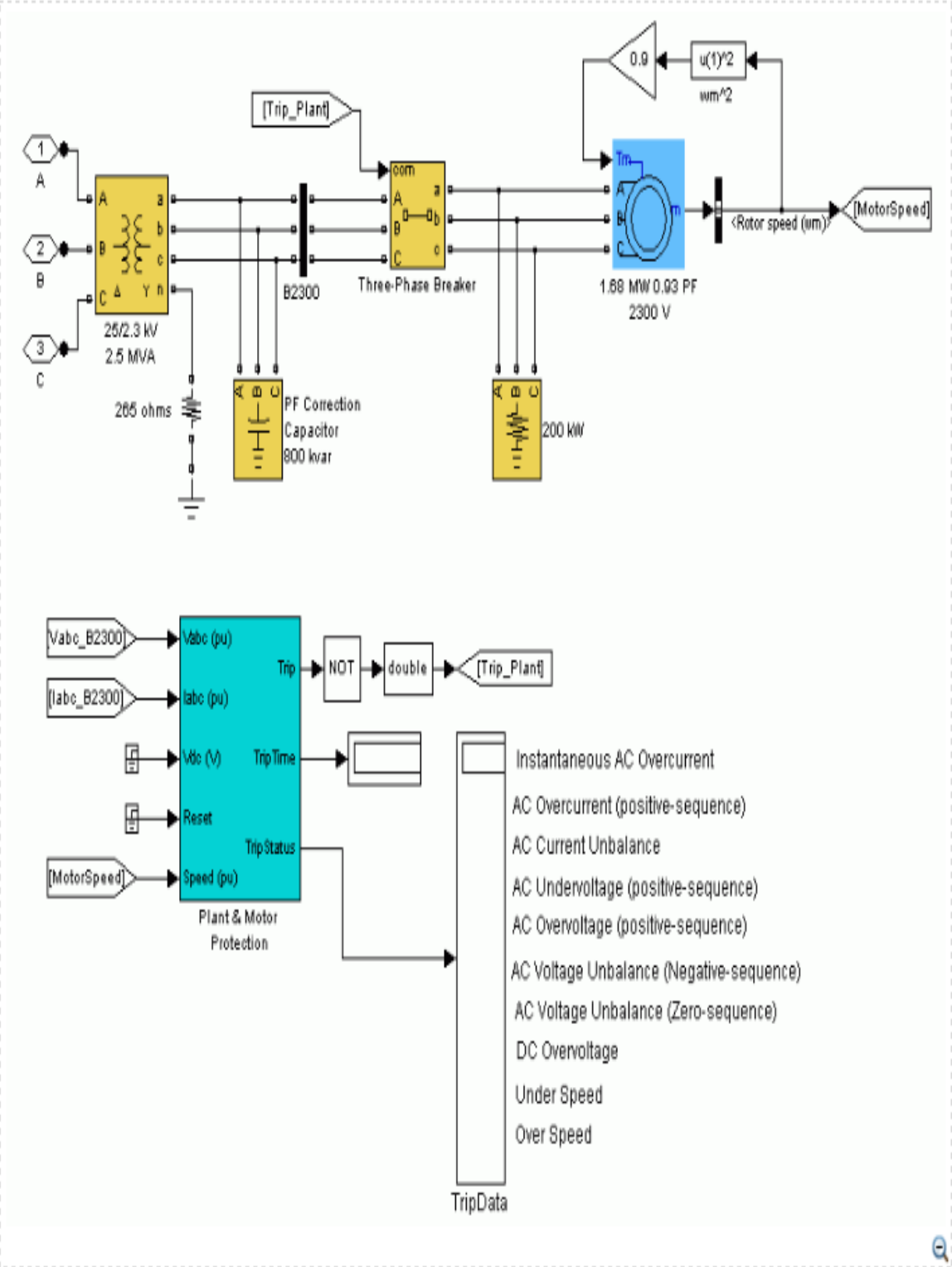

Figure 4.2: Plant with Its Protection System

4.4 Turbine Data Menu and the Turbine Power Characteristics

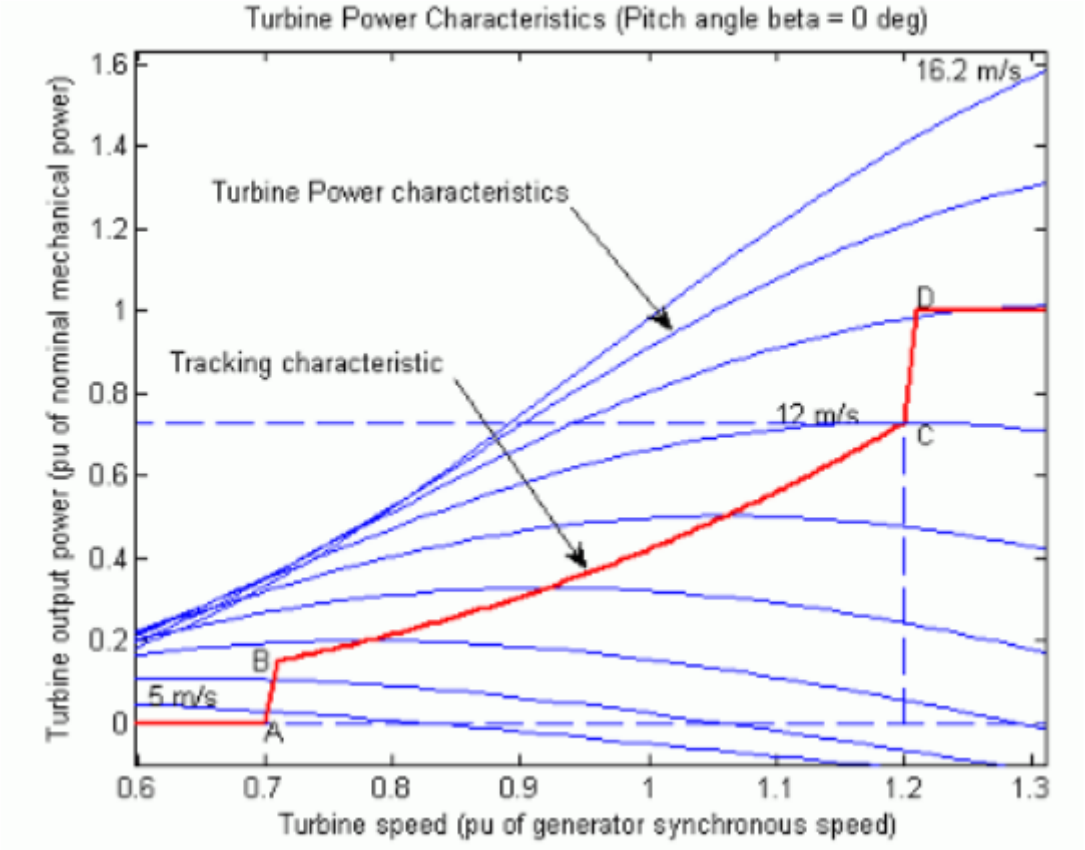

Figure 4.3: Turbine Data Menu and the Turbine Power Characteristics

The DFIG is controlled to follow the ABCD curve in Turbine Data Menu and the Turbine Power Characteristics. Turbine speed optimization is obtained between point B and point C on this curve.

The wind turbine model is a phasor model that allows transient stability type studies with long simulation times. In this case study, the system is observed during 50 s. The 6-wind-turbine farm is simulated by a single wind-turbine block by multiplying the following three parameters by six, as follows:

- The nominal wind turbine mechanical output power: 6*1.5e6 watts, specified in the Turbine data menu
- The generator rated power: 6*1.5/0.9 MVA (6*1.5 MW at 0.9 PF), specified in the Generator data menu

- The nominal DC bus capacitor: 6*10000 microfarads, specified in the Converters data menu the mode of operation is set to Voltage regulation in the Control Parameters dialog box. The terminal voltage will be controlled to a value imposed by the reference voltage (V_{ref}=1 pu) and the voltage droop (Xs=0.02 pu).

4.5 Response to a Change in Wind Speed

Simulation has been run from initial speed 8m/s to final value 14m/s.

4.5.1 Wind Farm in Voltage Regulation Mode

Figure 4.5 represent The voltage at bus B575, showing that the voltage is kept constant at 1 pu because the control mode is set as (VOLTAGE REGULATION).the 1pu voltage is regulated by controlling the reactive power of the generator, we notice that the generator absorb 0.68MVR to produce 1pu of voltage.

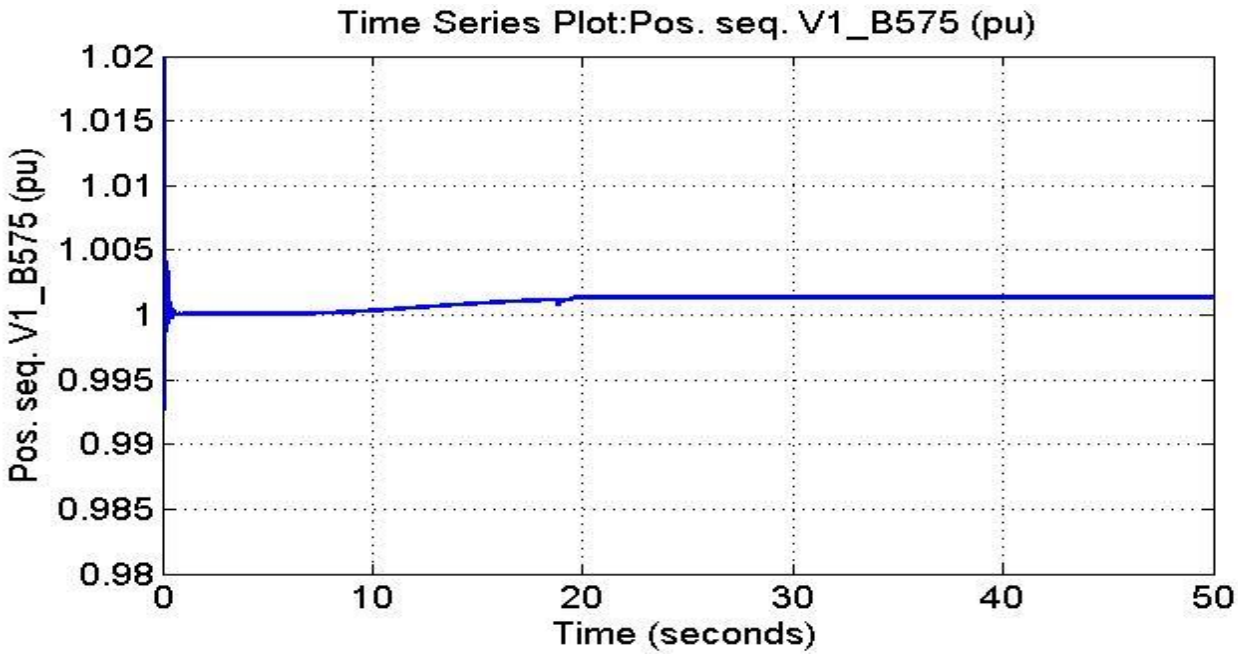

Figure 4.5: The positive sequence voltage at bus575 per unit

Figure 4.6 represent the current at bus B575, we notice that the initial current is 0.18 pu when t=5 the current started to increase gradually as result to increase in generated power at t=19 the current reached its rated value which is equal to 0.88 pu at the same time the power reached the rated value.

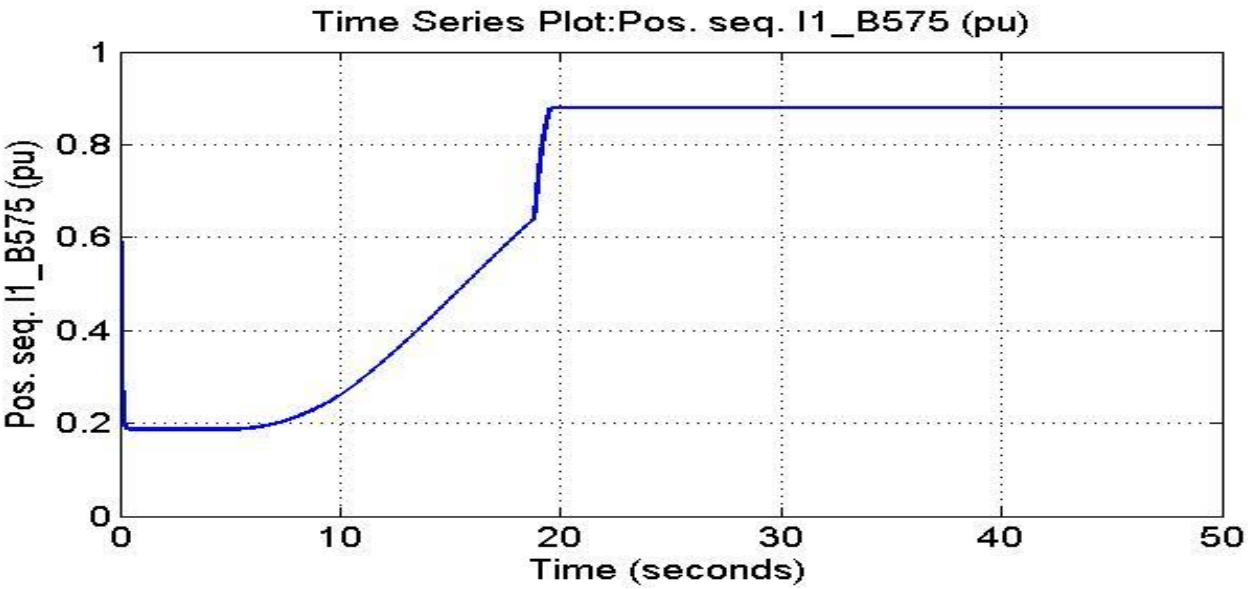

Figure 4.6: The positive sequence current at bus575 per unit

Figure 4.7 represent the generated active power in MW At t=5s the generated active power starts increasing smoothly (together with the turbine speed) to reach its rated value of 8.8 MW in approximately 15s.

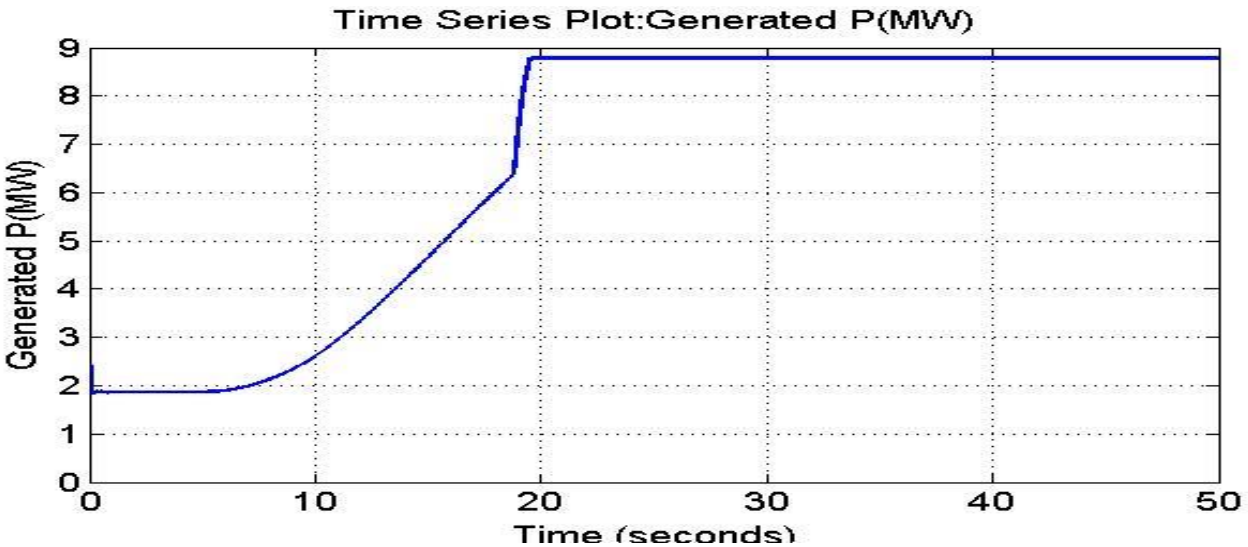

Figure 4.7: the generated active power

Figure 4.8 represent the generated reactive power in Mvar. Initially the Mvar is zero but at nominal power, the wind turbine absorbs 0.68 Mvar (generated Q=-0.68 Mvar) to control voltage at 1pu.

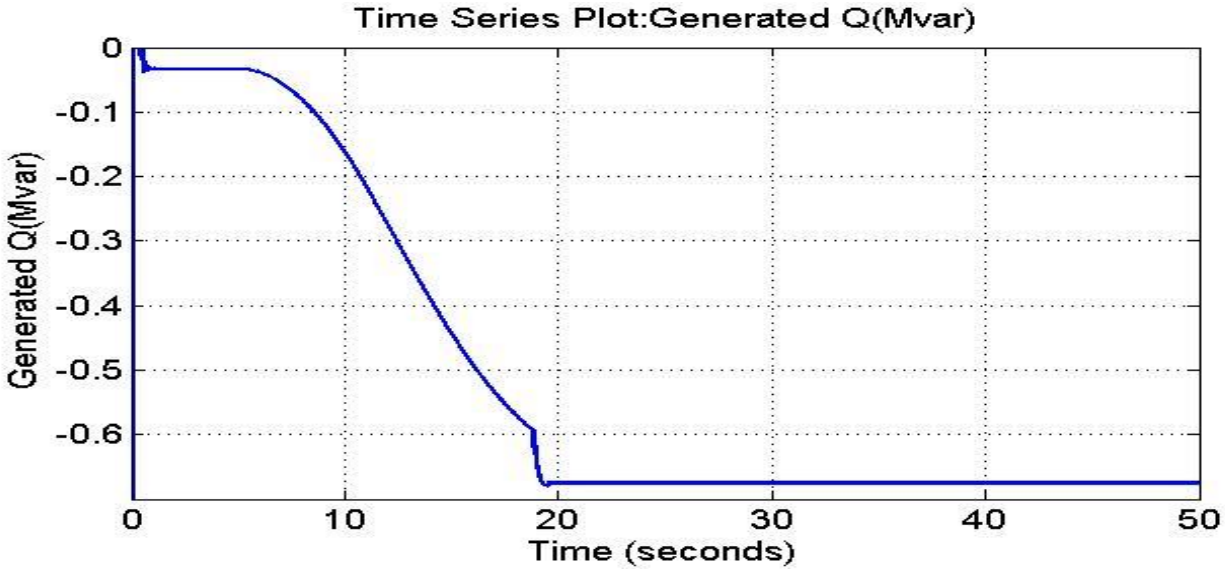

Figure 4.8: The generated reactive power

Figure 4.9 represent the dc link voltage in volt, the reference voltage is set at 1200 v ,and the control system regulate the voltage around this value .we notice small increase in voltage (voltage equal 1202v) at the same time when the generated power reached the rated value then the system return to steady state (voltage equal 1200).

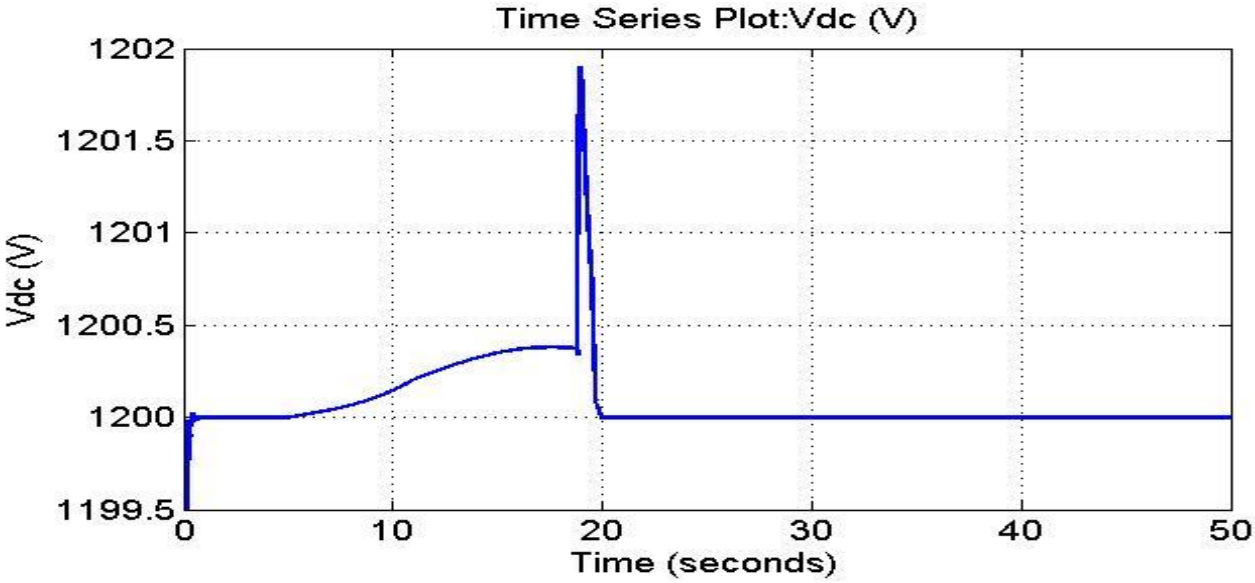

Figure 4.9: Dc link voltage

Figure 4.10 represent the generator speed in pu, the turbine speed increases from 0.8 pu to 1.21 pu. Initially, the pitch angle of the turbine blades is zero degree and the turbine operating point follows the red curve of the turbine power characteristics up to point D. Then the pitch angle is increased from 0 deg to 0.76 deg to limit the mechanical power.

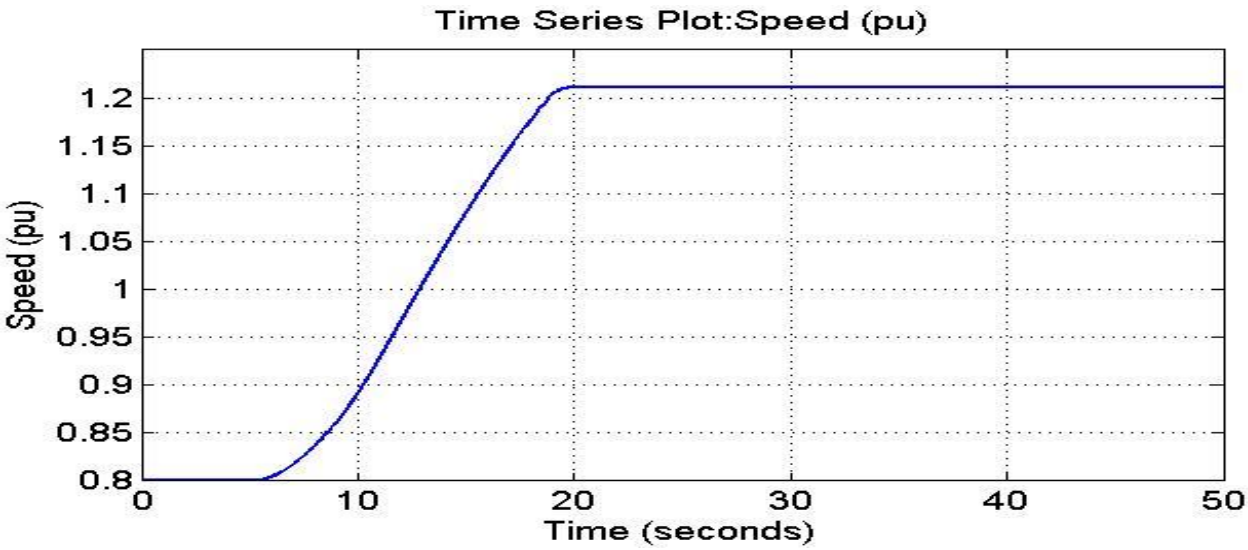

Figure 4.10: Turbine speed

Figure 4.11 represent the wind speed (m/s) in form of step function. Initially, wind speed is set at 8 m/s, and then at t=5s, wind speed increases suddenly at 14 m/s.

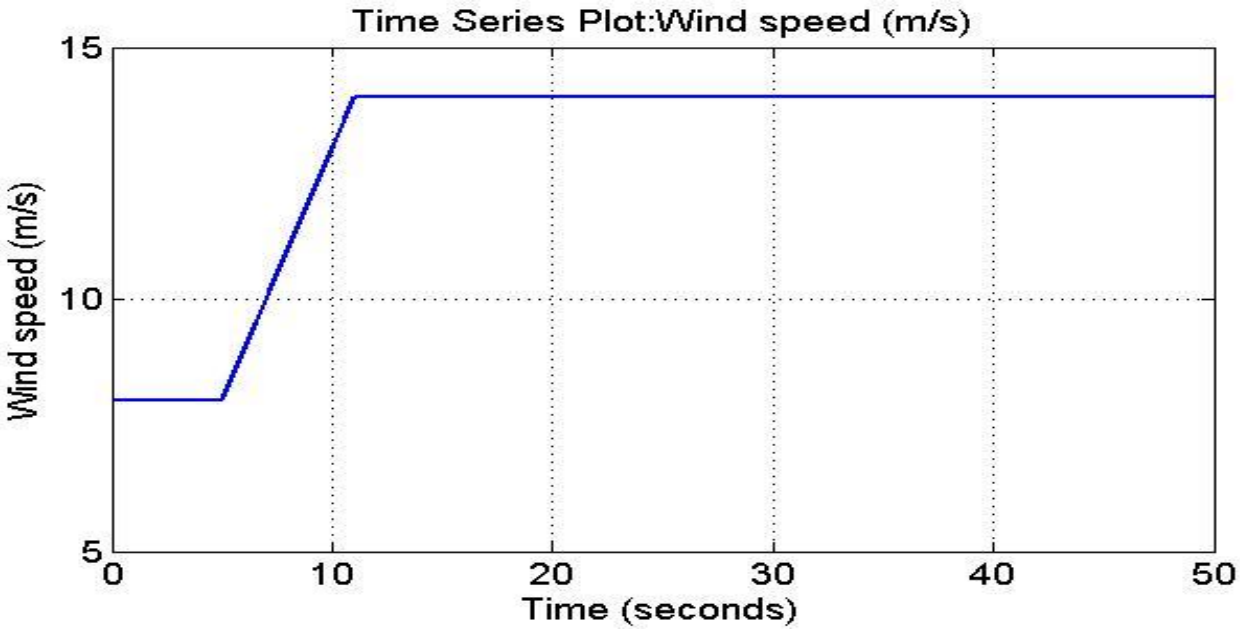

Figure 4.11: Wind speed

Figure 4.12 represent pitch angle in degree initially, the pitch angle of the turbine blades is zero degree and the turbine operating point follows the red curve of the turbine power characteristics up to point D. Then the pitch angle is increased from 0 deg to 0.76 deg to limit the mechanical power.

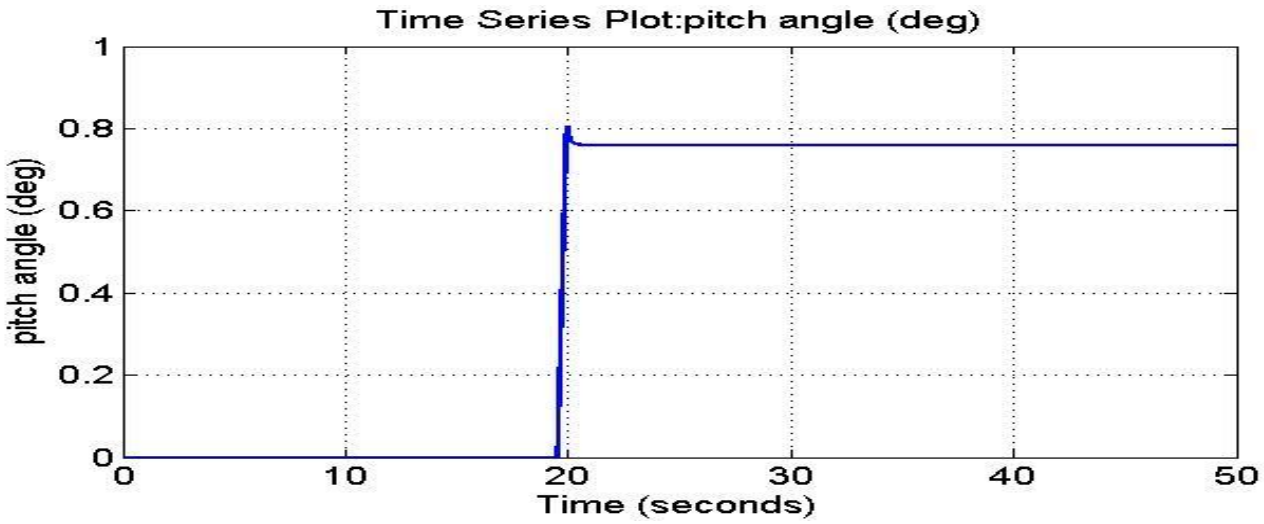

Figure 4.12: Pitch angle

4.5.2 Wind Farm in Var Regulation Mode

When changing the mode of operation to Var regulation with the Generated reactive power Qref set to zero, the voltage will increases to 1.021 pu when the wind turbine generates its nominal power at unity power factor.

Figure 4.13 represent the positive sequence voltage at bus575 per unit when control mode is changed to (var regulation) ,the voltage raised from 1 pu to 1.02 pu.

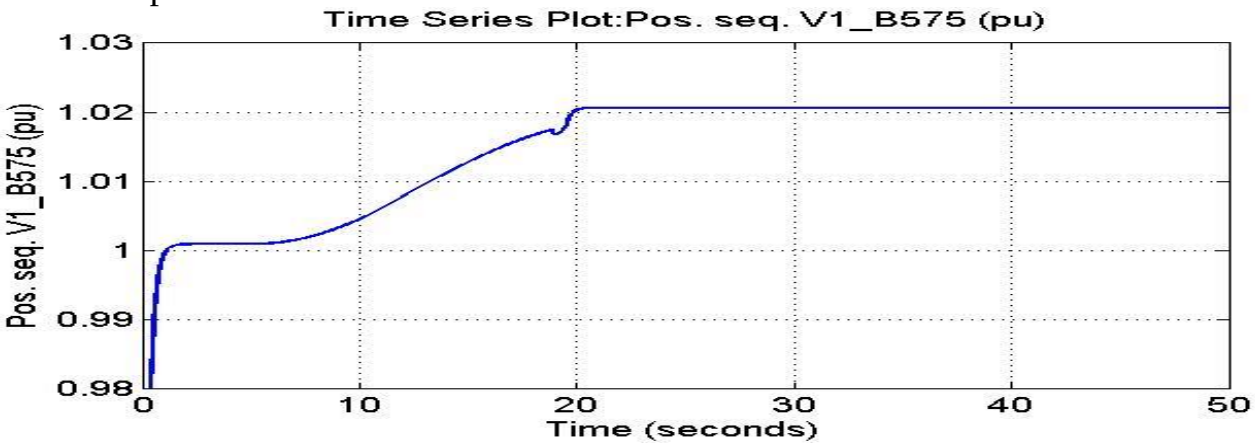

Figure 4.13: The positive sequence voltage at bus575 per unit

Figure 4.14 represent the generated reactive power, the control system tend to regulate the reactive power around the reference MVR .which is equal to (Qref=0).

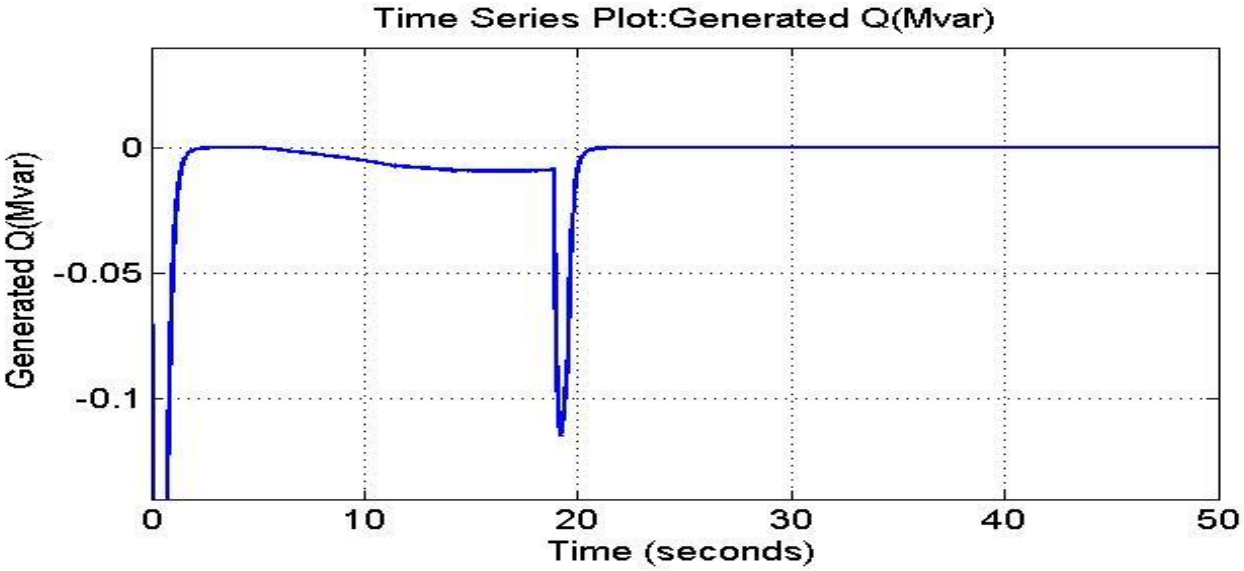

Figure 4.14: The generated reactive power

4.6 Response To Voltage Sag on The 120 kV System

Now observing the impact of a voltage sag that resulting from a remote fault on the 120-kV system. First, in the wind speed step block, the wind speed step has been disabled by changing the Final value from 14 to 8 m/s. the 120-kV voltage source menu has been opened, in the parameter "Time variation of", select “Amplitude". A 0.15 pu voltage drop lasting 0.5 s is programmed to occur at t = 5 s.

4.6.1 Wind Farm in Var Regulation Mode

Figure 4.15 illustrates the plant voltage sage. Initially the voltage is 1 pu, at t=5 sec the voltage drop 0.85, at t = 5.22 s, the protection system trips the plant because an under voltage lasting more than 0.2 s has been detected.

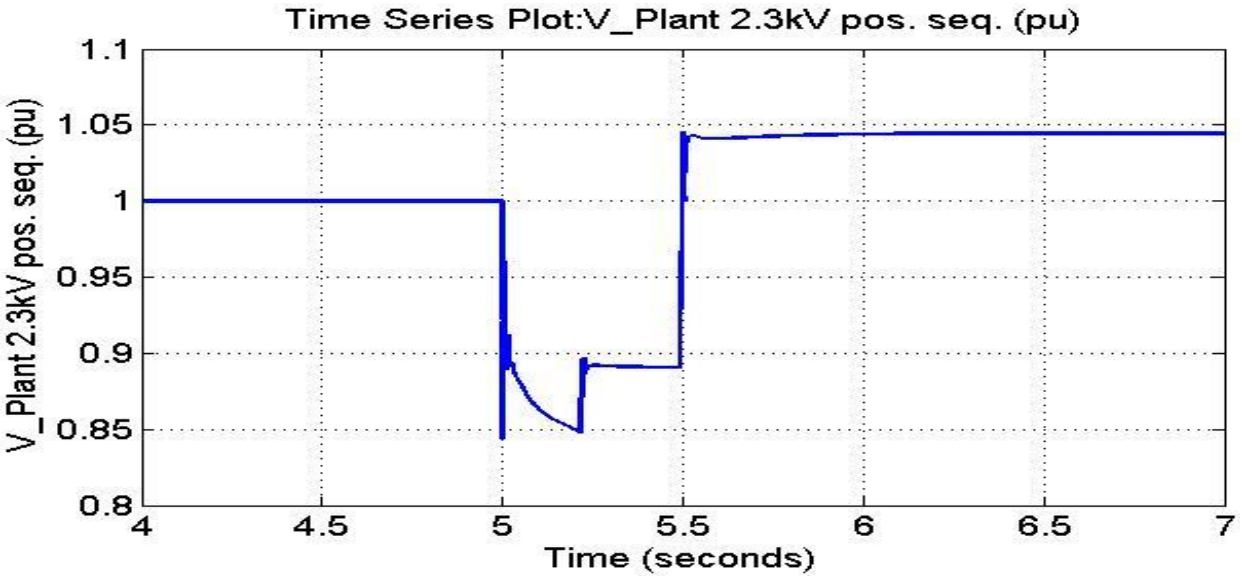

Figure 4.15: Plant voltage

Figure 4.16 illustrates the plant current, initially the plant absorb0.965 pu current, at t=5.22 sec the protection system trips the plant and the current absorbed falls to zero.

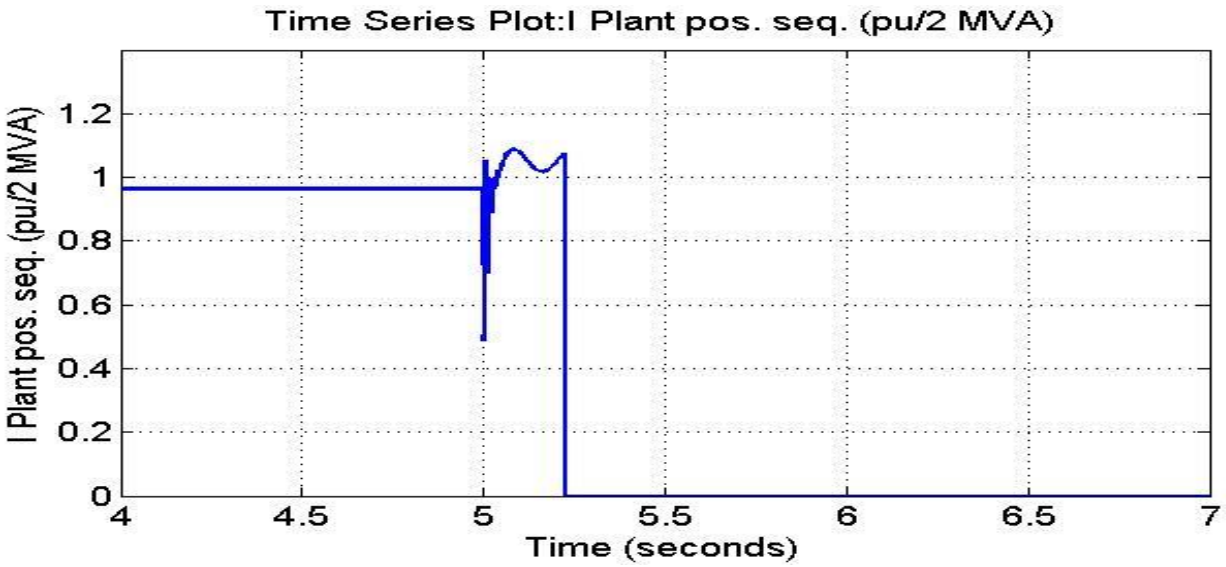

Figure (4.16) plant current

Figure 4.17 illustrates the motor speed, when the protection system trips the motor speed decreases gradually.

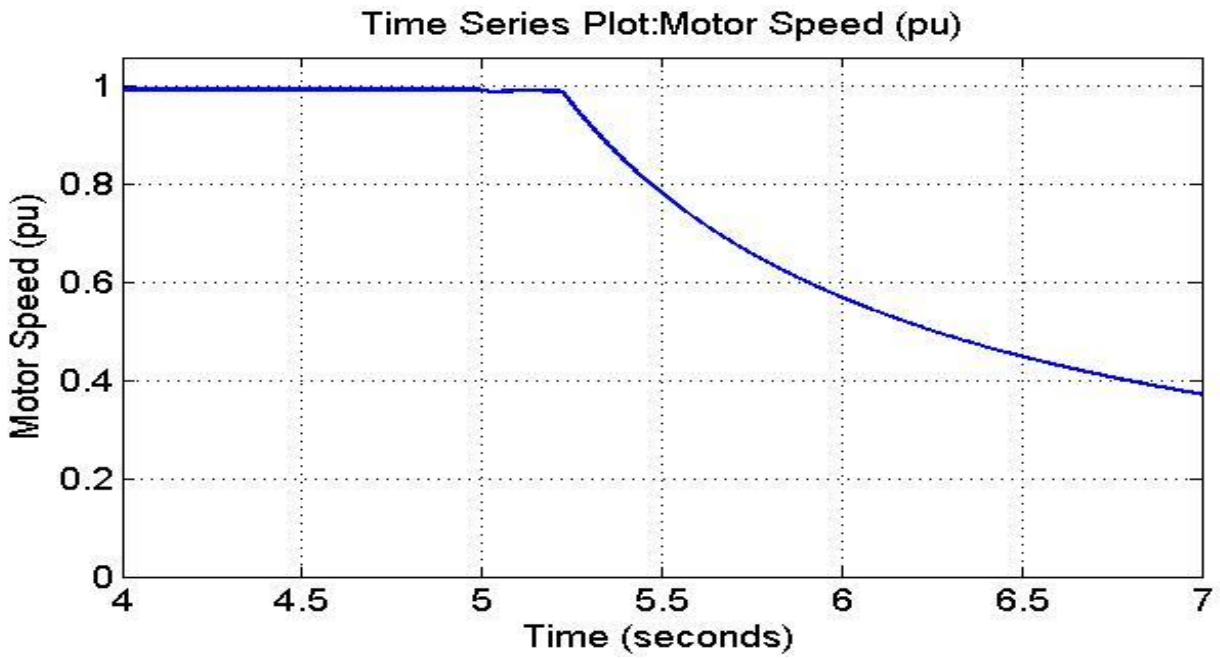

Figure (4.17):motor speed

Figure 4.18 illustrates the generated power and we notice that the wind farm produces 1.87 MW, also there is power oscillation from t=5 to t=5.5 then the power settled at 1.87 MW.

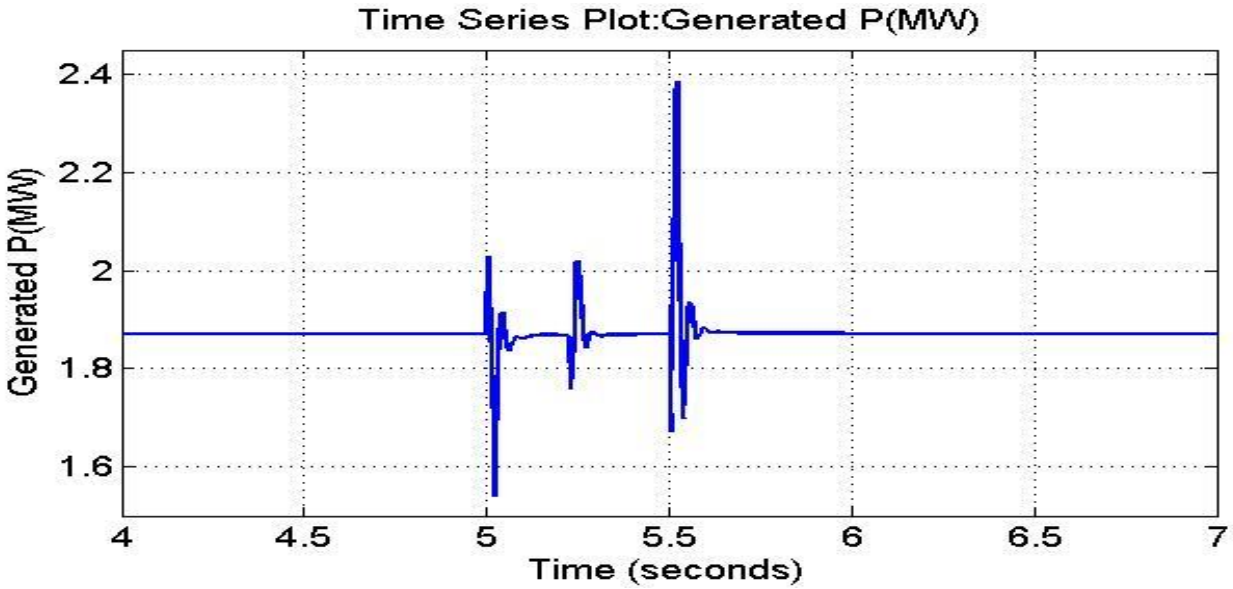

Figure 4.18: generated power

Figure 4.19 illustrates the power at bus B25. The initial power is 0.55 MW then at t=5.22sec the power falls to -1.25MW (1.25 MW is exported to the grid.) after the protection system has tripped the plant.

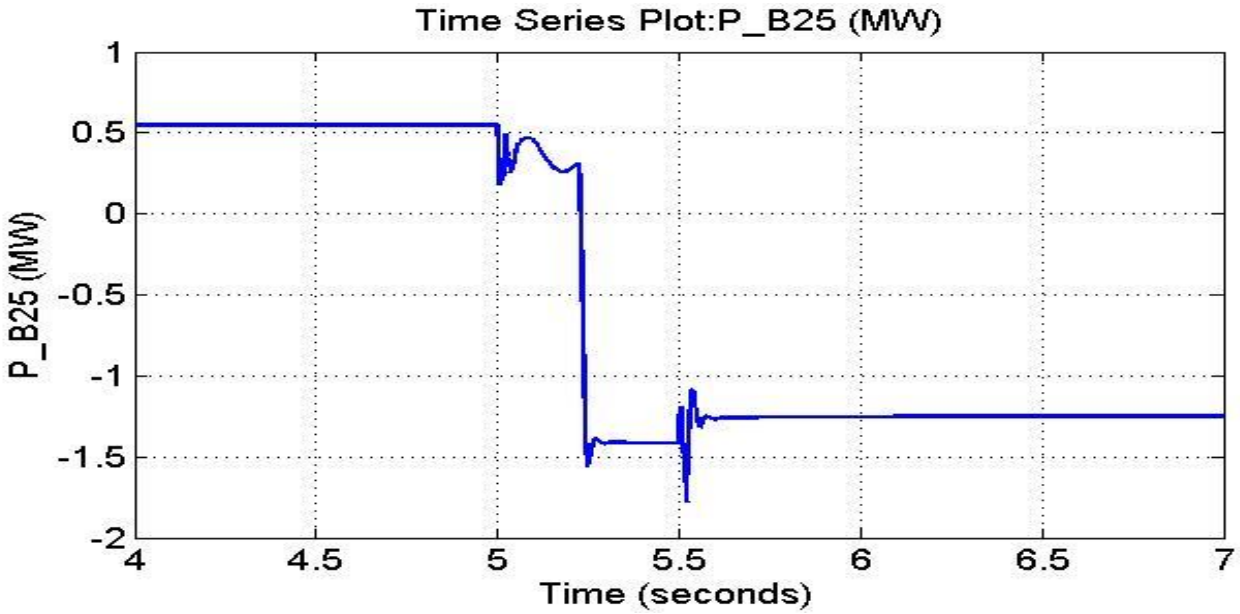

Figure 4.19: power at bus B25

4.6.2 Wind Farm in Voltage Regulation Mode

Figure 4.20 illustrates the plant voltage sage. Initially the voltage is 1 pu, at t=5 sec the voltage drop 0.85, at t = 5.22 s, the plant does not trip anymore. This is because the voltage support provided by the 5 Mvar reactive power generated by the wind-turbines during the voltage sag keeps the plant voltage above the 0.9 pu protection threshold. The plant voltage during the voltage sag is now 0.93 pu. After t=5.5 the voltage is regulated at 1 u.

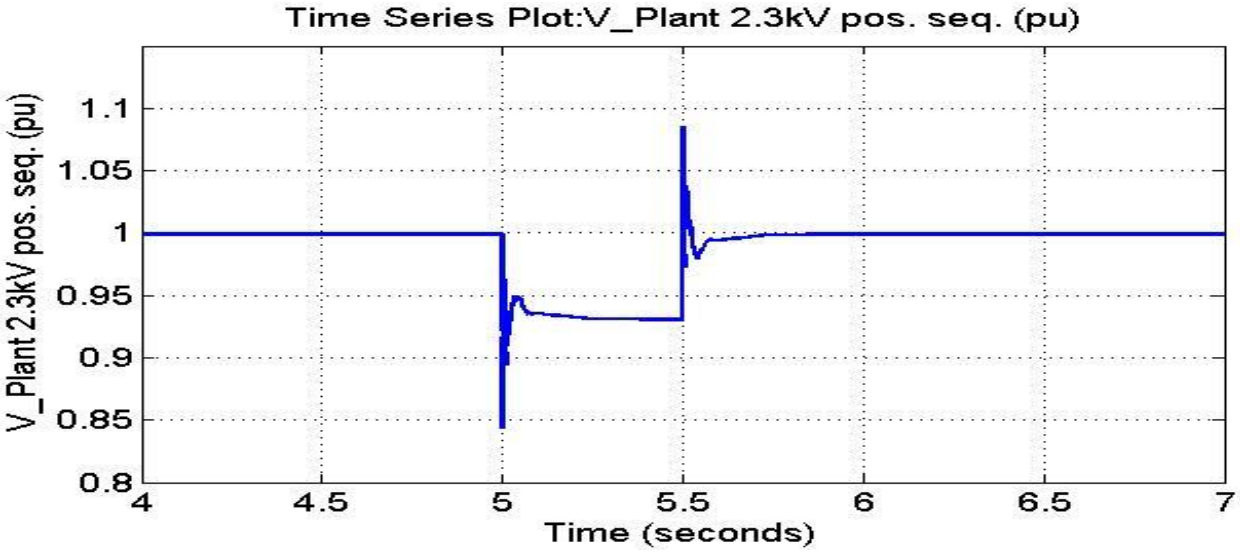

Figure 4.20: plant voltage

Figure 4.21 illustrates the plant current we notice that the plant still absorbing 0.96 pu and the protection system doesn't trip.

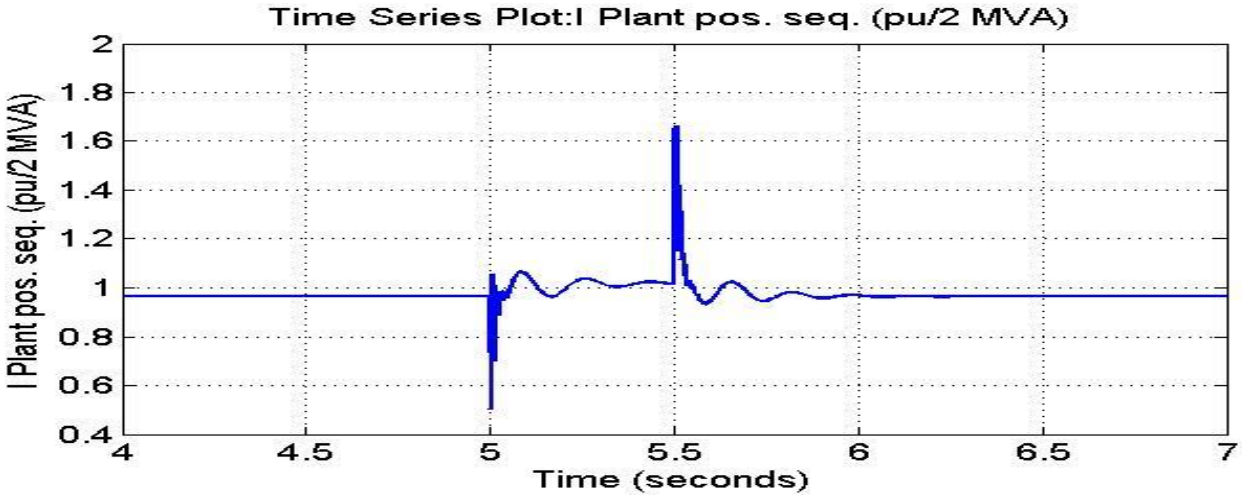

Figure 4.21: plant current

Figure 4.22 illustrates the motor speed, when the voltage sag occur we notice small oscillation in motor speed from t=5sec to 6 sec, after that the motor continue to run at constant speed 0.992 pu.

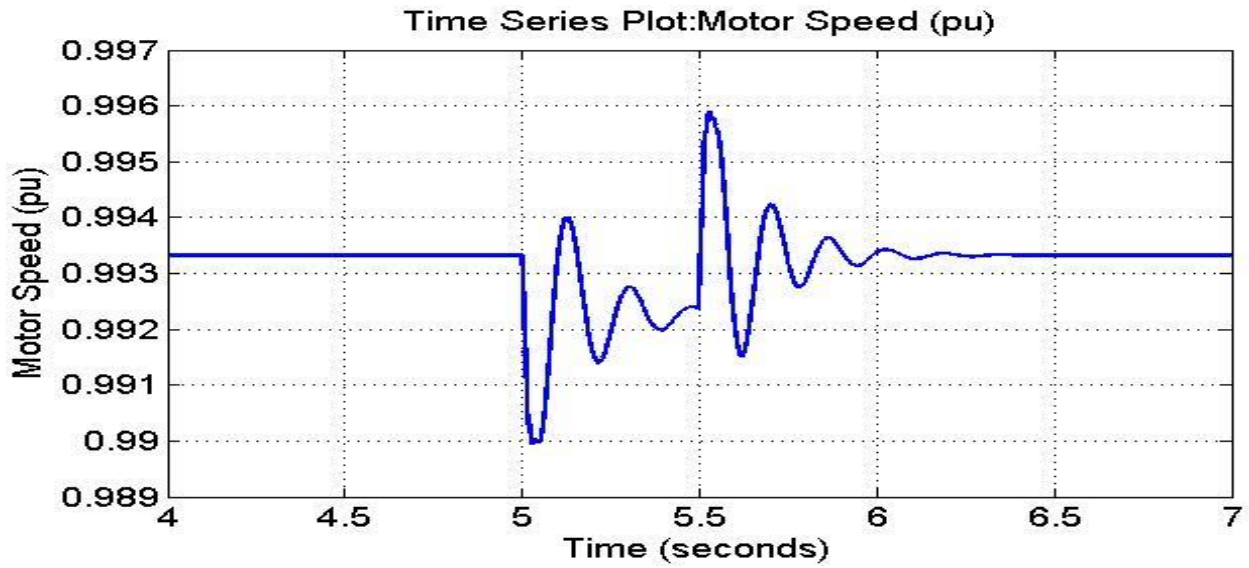

Figure 4.22: motor speed

Figure 4.23 illustrates the generated power and we notice that the wind farm produces 1.87 MW, also we notice power oscillation from t=5 to t=5.5 then the power settled at 1.87 MW.

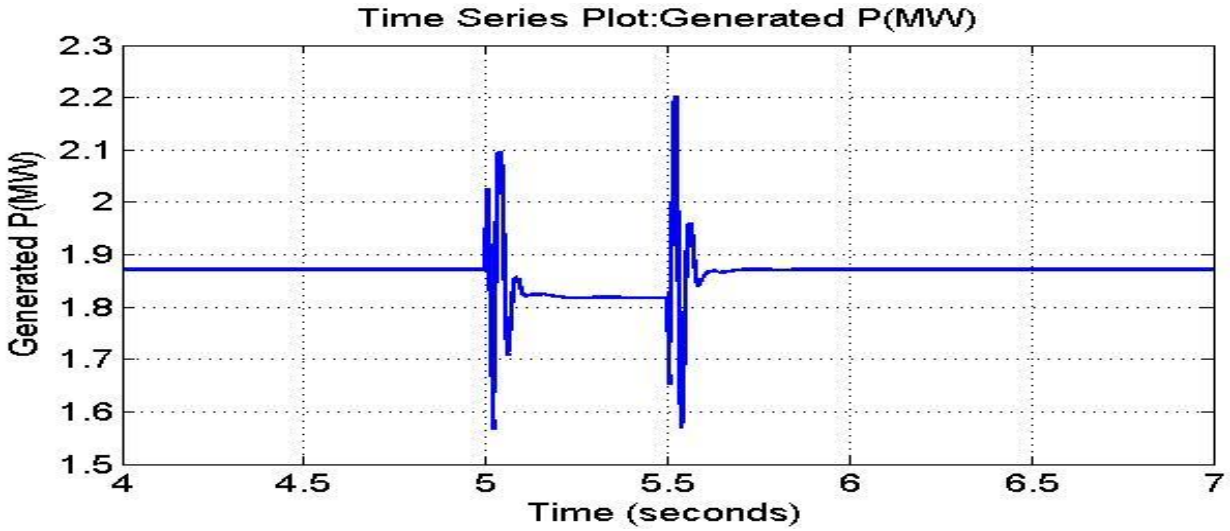

Figure 4.23: generated power

Figure 4.24 illustrates the power at bus B25, the bower is 0.55 MW and the motor continues to run.

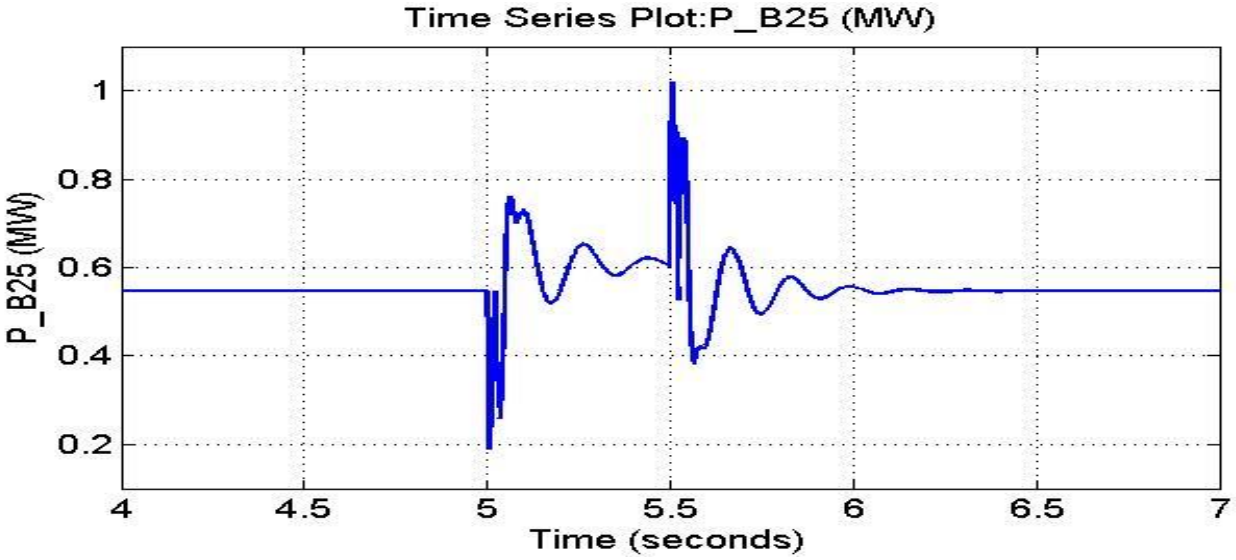

Figure 4.24: power at bus B25

4.7 Response To Fault on The 25 kV System

Now observe the impact of a single phase-to-ground fault occurring on the 25 kV line. At t=5 s a 9 cycle (0.15 s) phase-to-ground fault is applied on phase A at B25 bus.

4.7.1 Wind Farm in voltage Regulation Mode

Figure 4.25 illustrates the voltage at bus B575 ,The positive sequence voltage

at wind turbine terminals (V1_B575) drops to 0.8 pu during the fault, which is above the under voltage protection threshold (0.75 pu for a t>0.1 s).The wind farm therefore stays in service.

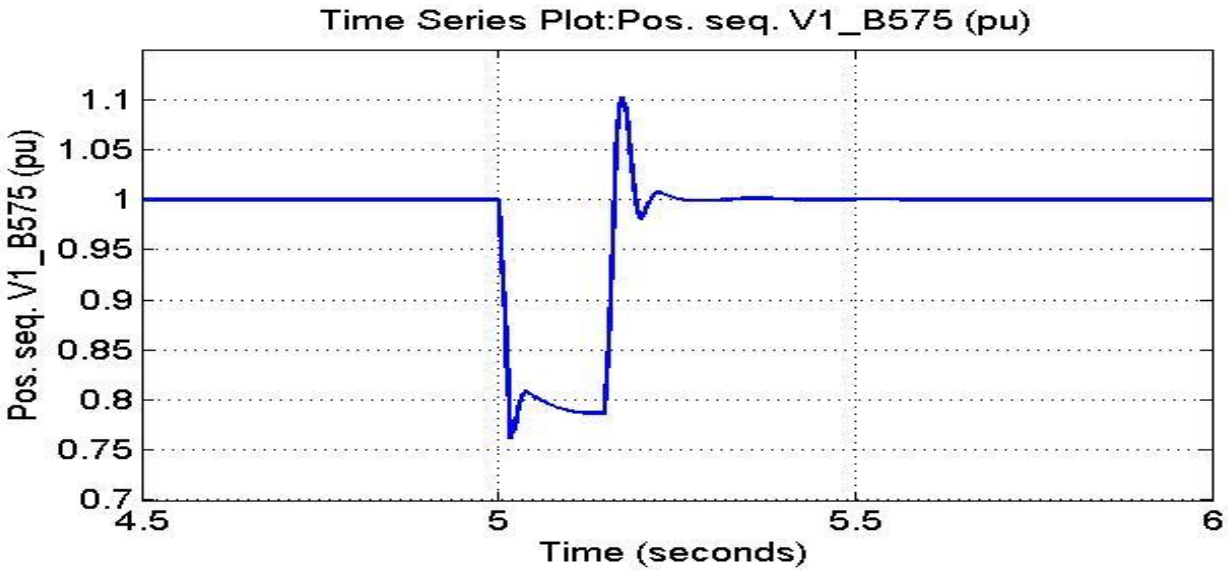

Figure 4.25: voltage at bus B575

Figure 4.26 illustrates the current at busB575, initially the current is 0.19 pu whet single phase to ground fault occur at t=5 sec the current rise suddenly to 0.7pu then at t=5.22sec the current once again returns to 0.19 pu. And the system doesn't trip.

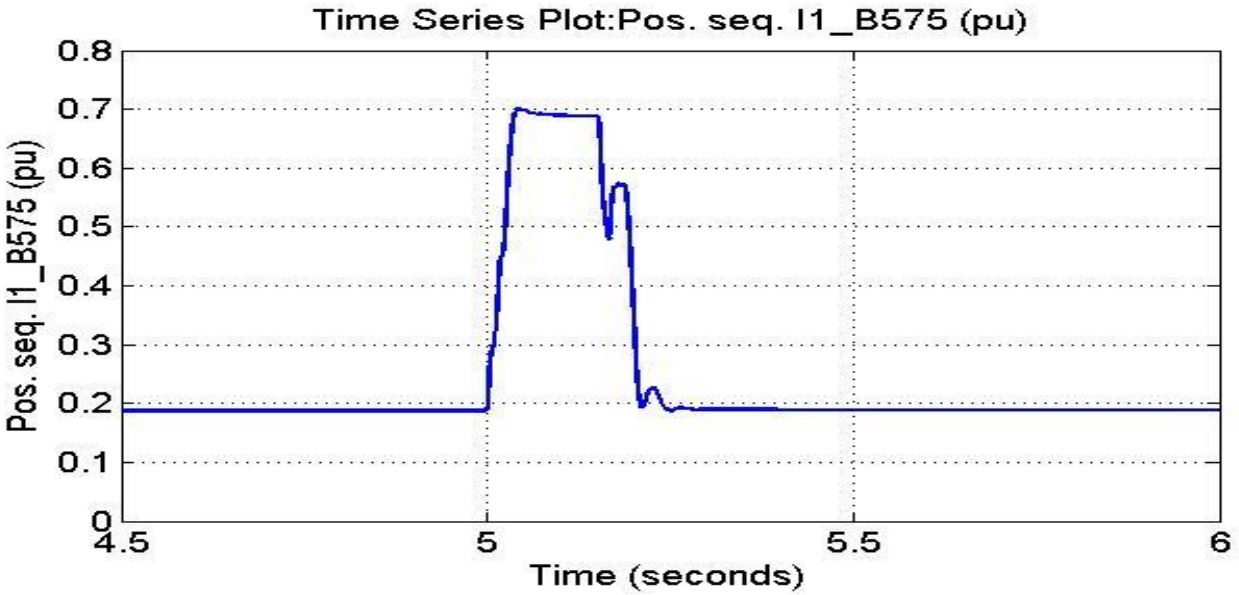

Figure 4.26: current at bus B575

Figure 4.27 illustrates the turbine speed, the turbine operate at constant speed (8 m/s).

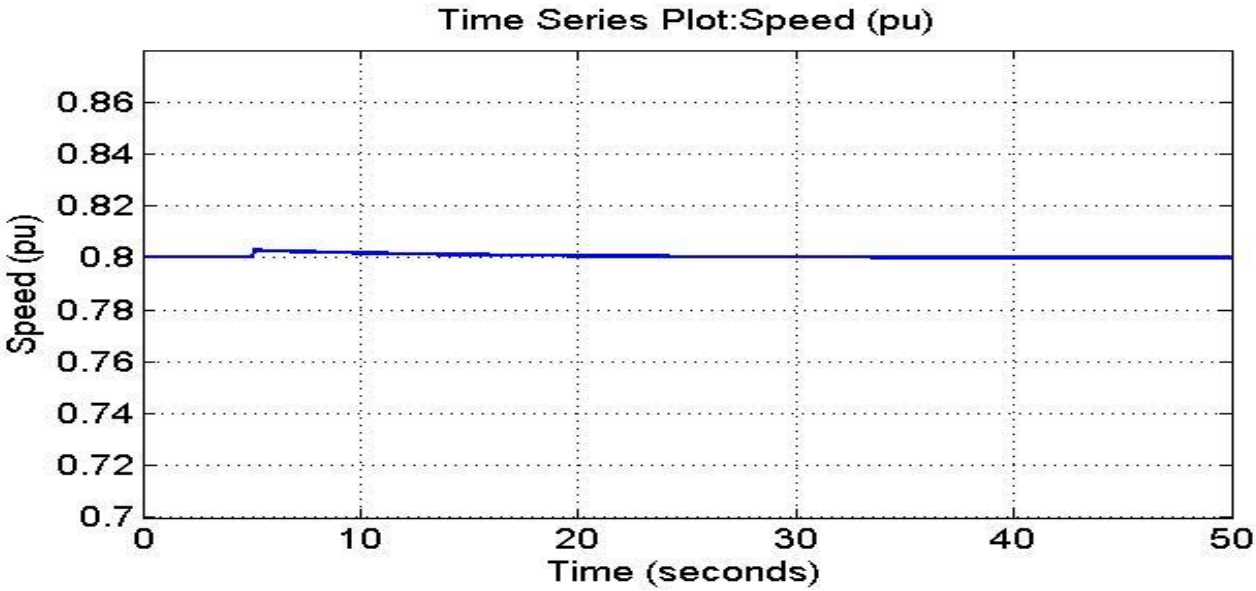

Figure 4.27: wind speed

Figure 4.28 illustrates the pitch angle control, the pitch angle is zero and there is no need to limit the speed.

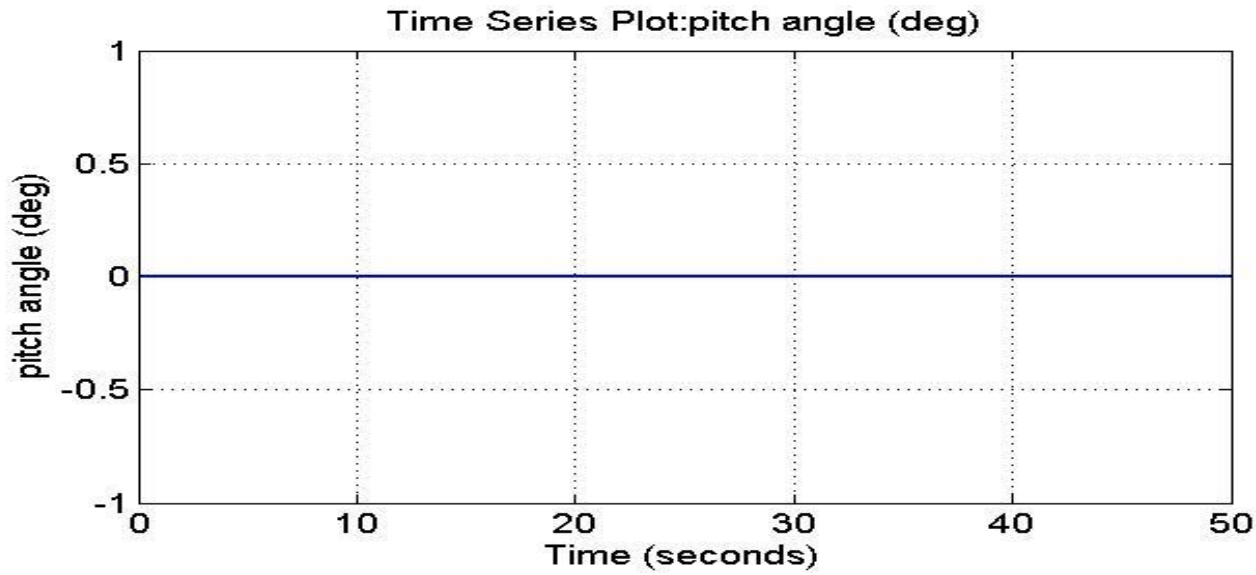

Figure (4.28): pitch angle

4.7.2 Wind Farm in Var Regulation Mode

Figure 4.29 illustrates the voltage at bus B575, if the Var regulation mode is used with Qref=0, the voltage drops under 0.7 pu and the under voltage

protection trips the wind farm.

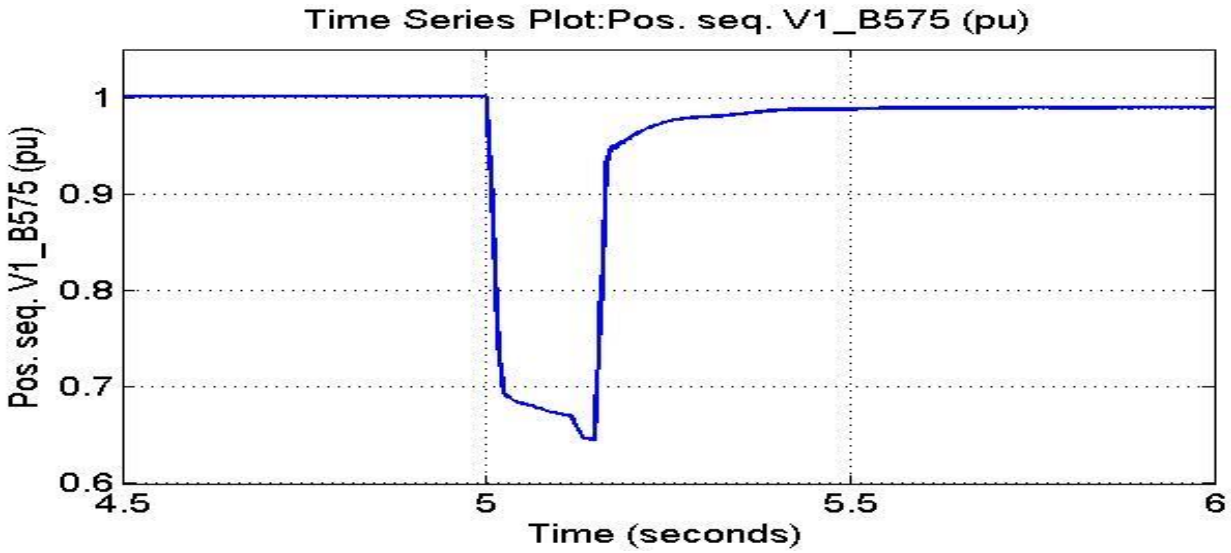

Figure (4.29): voltage at bus B575

Figure 4.30 illustrates the current at busB575, initially the current is 0.19 pu whet single phase to ground fault occur at t=5 sec the current rise suddenly to 0.29 pu then at t=5.22sec the current goes to zero because the protection system tripped the wind farm.

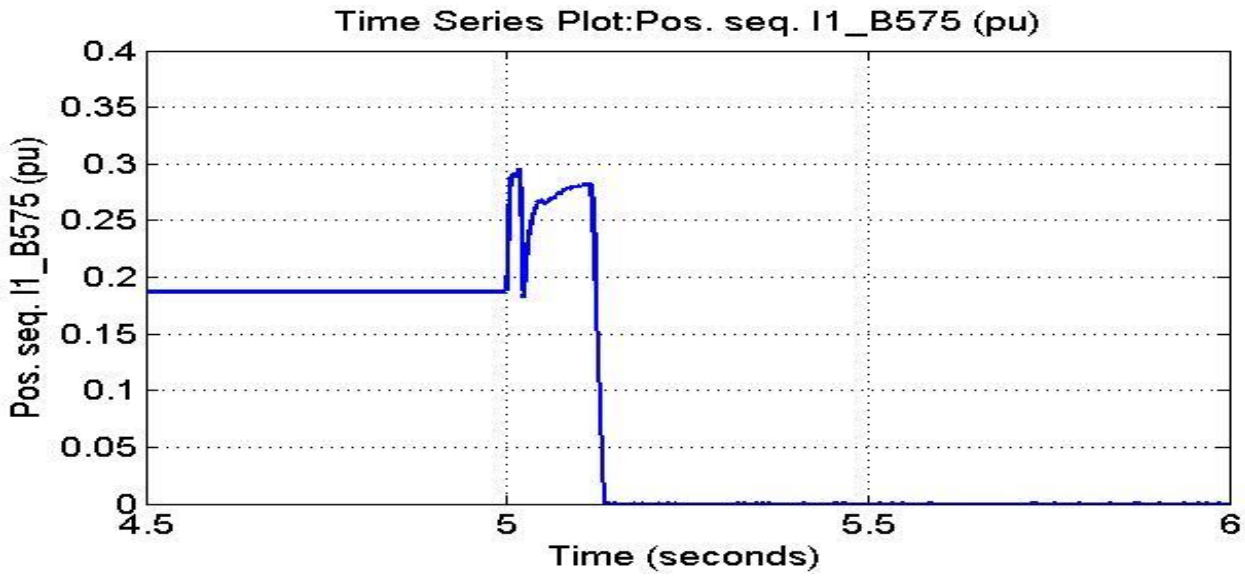

Figure (4.30): current at bus B575

Figure 4.31 illustrates the turbine speed, the turbine operate initially at constant speed (8 m/s).when fault occur at t=5 sec the turbine speed started to increase gradually ,which will cause a major mechanical stress on the turbine blades ,

this mechanical stress can destroy the turbine blades.

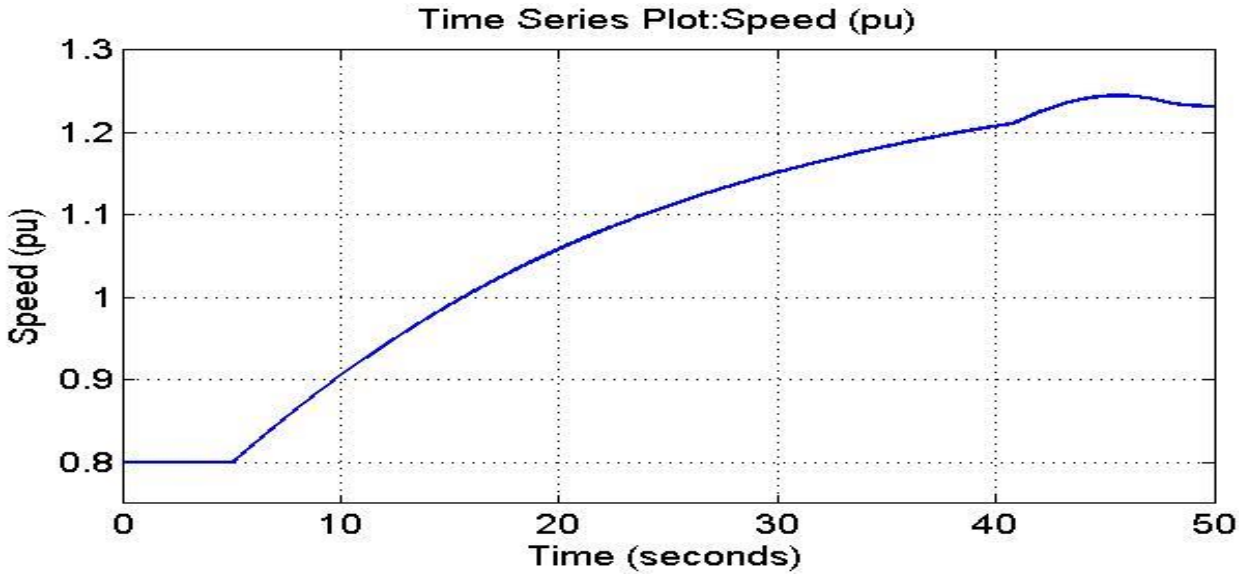

Figure (4.31): turbine speed

Figure 4.32 illustrates the pitch angle control initially the blade pitch angle is zero, at t=40 s the pitch angle starts to increase to limit the speed.

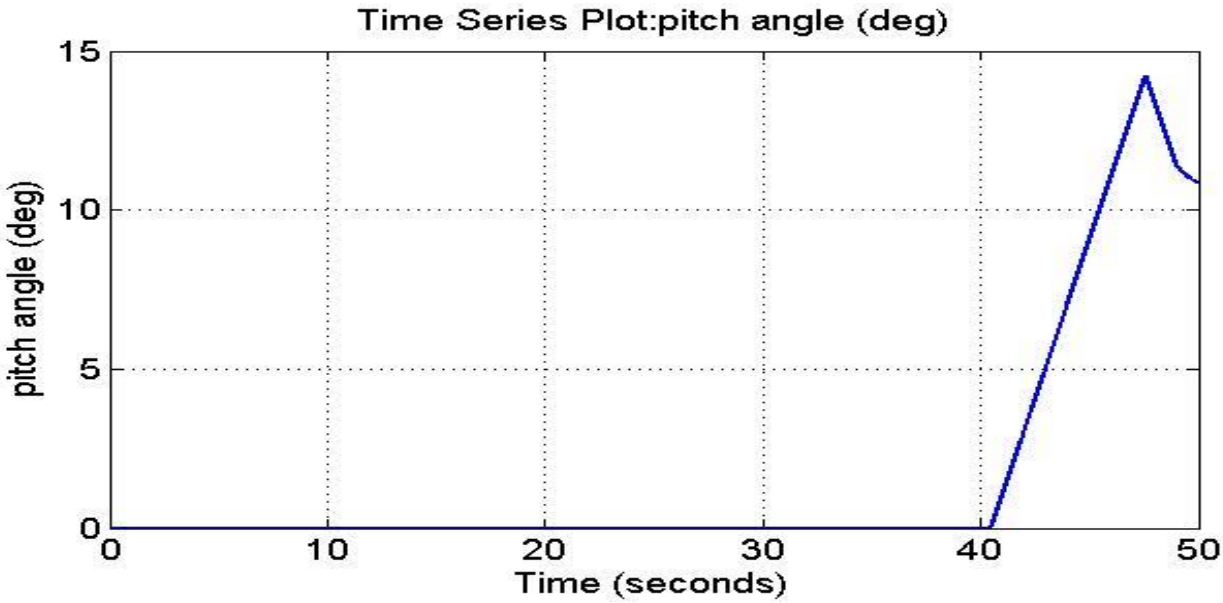

Figure (4.32): pitch angle

CHAPTER FIVE

CONCLUSION AND RECOMMENDATIONS

5.1 CONCLUSION

We have discussed here the basic operation of DFIG and its control using AC/DC/AC converter. First, Wind turbine and double fed induction generator have been modeled. For best efficiency the DFIG system is used which is connected to grid side and has better control. The rotor side converter (RSC) usually provides active and reactive power control of the machine while the grid-side converter (GSC) keeps the voltage of the DC-link constant. So finally we simulated grid side and wind turbine side parameters and the corresponding results have been displayed. The model is a discrete-time version of the Wind Turbine Doubly-Fed Induction Generator (Phasor Type) of Matlab/Sim Power Systems. Here we also took the protection system in consideration which gives a trip signal to the system when there is a fault (single phase to ground fault) on the system. The faults can occur when wind speed decreases to a low value or it has persistent fluctuations. The DFIG is able to provide a considerable contribution to grid voltage support during short circuit periods. Considering the results it can be said that doubly fed induction generator proved to be more reliable and stable system when connected to grid side with the proper converter control systems.

5.2 Recommendations:

- For future studies for those who have an interest in wind power may try to study and analysis wind farm based on variable speed synchronous generator.
- Applying more transient cases.
- Develop various studies such as interaction of wind farm with an energy storage system.
- Interaction of model with a solar system.

REFERENCES

[1] L. Abdallah and T. El-Shennawy, "Reducing Carbon Dioxide Emissions from Electricity Sector using Smart Electric Grid Applications", Web. 2012.

[2]- "Renewable energy shows strongest growth in global electric generating capacity," U.S. Energy Information Administration, SEPTEMBER 28, 2011, Available athttp://www.eia.gov/todayinenergy/detail.cfm?id=3270 (Accessed: 28 January 2014).

[3] A. Shahab, "Dynamic Average-Value Modeling of Doubly-Fed Induction Generator Wind Energy Conversion Systems," Master Thesis, *the University of Manitoba*, 2013.

[4] Deshmukh, M. K., and C. Balakrishna Moorthy, "Review on Stability Analysis of Grid Connected Wind Power Generating System," *International Journal*, 2013.

[5] S. Arnaltes, "Comparison of Variable Speed Wind Turbine Control Strategies", Proceedings of the International Conference on Renewable Energies and Power Quality,
Vigo (Spain), April 2003.

[6] O. Silva, H. Dayarathne, V. Dasanayake, J. Silva and A.Rodrigo, "Wind Generator Dynamics: Modeling of Fixed Speed Asynchronous Wind Generator using PSS/E," October 31, 2013.

[8] National Instruments, "Wind Turbine Control Methods," December 22, 2008, Available at http://www.ni.com/white-paper/8189/en/#toc1 (Accessed:9 February 2014).

[9]-Mukund_R._Patel_"Wind_and_solar_power_systems"de (BookZZ.org) U.S. Merchant Marine Academy Kings Point, New York, U.S.A. Second Edition.

[11]-Mohammad Rashed M. Altimania modeling of doubly-fed induction generators connected to distribution system based on emegasim® real-time digital simulator.

[12]-Mohammed Omer Mohammed, "Maximum power point traker of wind energy generation systems", thesis of MSc. in Sudan University of science and technology, September 2015.